Published for SISSA by Springer

Received: *October 29, 2025*
Revised: *April 25, 2026*
Accepted: *April 27, 2026*
Published: *July 3, 2026*

Search for single production of a vector-like T quark decaying to a top quark and a neutral scalar boson in the lepton+jets final state in proton-proton collisions at $\sqrt{s} = 13$ TeV

The CMS collaboration

Full author list at the end of the paper

E-mail: cms-publication-committee-chair@cern.ch

Abstract: A search for single production of a vector-like T quark with charge $2e/3$, decaying to a top quark and a neutral scalar boson is presented. The boson can be a standard model Higgs boson (H) or a new scalar boson (ϕ). In the first case, a branching fraction of 25% is assumed for the decay $\mathrm{T} \to \mathrm{tH}$, while in the second case the T quark is assumed to decay exclusively to $\mathrm{t}\phi$. The top quark is identified via its lepton+jets decay, and the neutral boson via its decay into a bottom quark-antiquark pair. Final states with Lorentz-boosted topologies are considered and machine-learning techniques are exploited for optimal event classification. The analysis uses data collected by the CMS experiment in proton-proton collisions at a center-of-mass energy of 13 TeV, corresponding to an integrated luminosity of 138 fb^{-1} recorded at the CERN LHC in 2016–2018. Upper limits at 95% confidence level are set on the product of cross section and branching fraction for a T quark in a narrow-width approximation. They vary between 14.7 and 0.1 fb, for T quark masses in the range 1.3–3.0 TeV and ϕ boson masses in the range 25–250 GeV. These are the first exclusion limits set on the production of a single T quark decaying into a top quark and a new neutral scalar boson. For the decay channel into a top quark and a standard model Higgs boson, the results provide the best limits on production cross sections to date, for T quark masses above 2 TeV.

Keywords: Hadron-Hadron Scattering, Top Physics, Vector-Like Quarks

ArXiv ePrint: 2510.25874

https://doi.org/10.1007/JHEP07(2026)041

JHEP07(2026)041

Contents

1 Introduction

Several extensions of the standard model (SM) predict the existence of heavy partners of SM quarks, referred to as vector-like quarks (VLQs) [1–7], which provide solutions to unresolved issues of the theory such as the large gap between the Planck scale and the electroweak scale, known as the hierarchy problem. These VLQs are colored spin-1/2 fermions with symmetric chirality under the electroweak gauge symmetry group. Therefore, unlike the chiral quarks of the SM, VLQs do not receive their masses from Yukawa couplings. While precision SM measurements have put tight constraints on the existence of a fourth generation of chiral quarks [8], this is not the case for VLQs. At the CERN LHC, VLQs may be produced in pairs mainly via strong processes, or singly via electroweak processes. The latter mode dominates for VLQ masses above 1 TeV owing to the larger phase space.

This paper presents a search for the production of a single vector-like T quark with charge $2e/3$ in proton-proton (pp) collision data at $\sqrt{s} = 13\,\mathrm{TeV}$ collected with the CMS detector in 2016–2018 and corresponding to an integrated luminosity of $138\,\mathrm{fb}^{-1}$. The decay channels analyzed are $\mathrm{T} \to \mathrm{t}\phi$ and $\mathrm{T} \to \mathrm{tH}$ where t is a top quark, ϕ is a new neutral scalar boson, and H is the SM Higgs boson. An example of a leading-order (LO) Feynman diagram for single T quark production, where the T quark is produced in association with a bottom (b) quark in the final state (bTq production) is shown in figure 1, with the T quark decaying to $\mathrm{t}\phi$ or tH.

In minimal scenarios, which have been typically considered for VLQ searches, the T quark couples to third-generation SM quarks and weak bosons, leading to decay channels into a bottom quark and a W boson, or a top quark and a Z boson. It also couples to the Higgs boson, resulting in the tH decay. Branching fractions are a function of the model-dependent

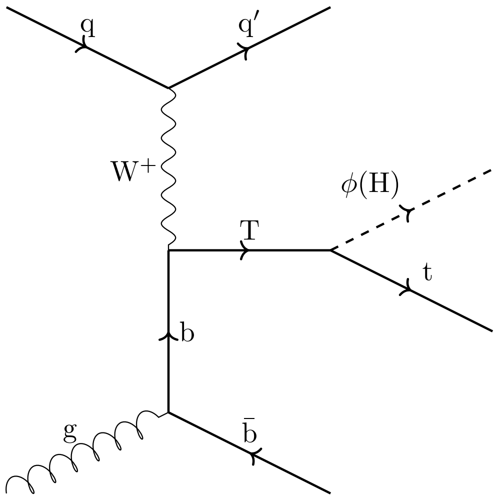

Figure 1. A representative leading-order Feynman diagram for the production of a single vector-like quark T decaying into a top quark and a neutral scalar boson, which may be a new scalar boson or an SM Higgs boson. Associated production with a bottom quark in the final state is shown.

values of the couplings. In this search, we assume a singlet T quark, which decays into tH with a branching fraction of 25% [1, 9]. A nonminimal scenario, where the T quark decays to a top quark and a beyond-the-SM scalar boson with a 100% branching fraction [10–12], is also considered in this search.

Recent reviews of VLQ searches in Run 2 of the LHC have been published by the ATLAS [13] and CMS [9] Collaborations. Searches for pair production of T quarks at a center-of-mass energy of 13 TeV, targeting a variety of possible final states, have been performed by ATLAS [14–23] and CMS [24–29]. Searches for single production of T quarks in the tH decay channel, exploiting fully hadronic final states, have also been reported by ATLAS [30] and CMS [31, 32]. A search in the tH and tZ channels using final states with one lepton has been published by ATLAS [33], while a search exploiting the diphoton decay mode of the Higgs boson has been published by CMS [34]. The tZ and bW decay channels have also been investigated, with results reported by both ATLAS [35–39] and CMS [40–42].

The search reported in this paper targets final states where the top quark decays in the lepton+jets channel via $\mathrm{t} \to \mathrm{Wb} \to \ell\nu\mathrm{b}$ and the scalar boson decays to a bottom quark-antiquark pair ($\mathrm{H}, \phi \to \mathrm{b\overline{b}}$). The experimental signature consists of one electron or muon (denoted as ℓ in this paper), the hadronization products of the b quarks, and a neutrino that is not reconstructed in the detector, causing an imbalance in the total transverse momentum (p_{T}) of the reconstructed events. As shown in figure 1, in addition to the bottom quark produced in association with the T quark, final states of signal events are also characterized by a light-flavor quark that tends to be emitted at a low angle with respect to the beam axis, in the forward region of the detector. Mass values in the 1–3 TeV range for the T quark, and 25–250 GeV for the ϕ boson, are considered in the analysis.

The analysis is designed to be sensitive to signatures with a large Lorentz boost of the T quark decay products. The ϕ boson is reconstructed as a large-radius jet, since in this regime the b quarks from its decay produce jets that tend to be collimated. Similarly, the lepton and jet from the top quark decay tend to overlap, which makes the top quark reconstruction more challenging. A top quark identification algorithm, based on machine-learning techniques, has been developed for this analysis in order to optimize the identification efficiency for the top quark decay.

For the interpretation of search, a singlet T quark model [5] is assumed, in which the production process is associated bTq production. This process has a much larger cross section than the associated production with a top quark tTq, which is in fact suppressed because of the higher masses of top quark as compared to bottom quark [5], and is therefore not considered as part of the signal. However, no specific requirement on the associated top or bottom quark is considered in the analysis selection and strategy, and, by design, the results of this search may also be interpreted in terms of other models, such as composite Higgs or little Higgs models [6], with the same final state.

Tabulated results are provided in the HEPData record for this analysis [43].

2 The CMS detector, data, and simulation

The central feature of the CMS apparatus is a superconducting solenoid of 6 m internal diameter, providing a magnetic field of 3.8 T. Within the solenoid volume are a silicon pixel and strip tracker, a lead tungstate crystal electromagnetic calorimeter (ECAL), and a brass and scintillator hadron calorimeter (HCAL), each composed of a barrel and two endcap sections. Forward calorimeters extend the pseudorapidity coverage provided by the barrel and endcap detectors. Muons are measured in gas-ionization detectors interleaved with the layers of the steel flux-return yoke outside the solenoid. More detailed descriptions of the CMS detector, together with a definition of the coordinate system used and the relevant kinematic variables, can be found in refs. [44, 45].

Events of interest are selected using a two-tiered trigger system. The first level (Level-1), composed of custom hardware processors, uses information from the calorimeters and muon detectors to select events at a rate of around 100 kHz within a fixed latency of 4 μs [46]. The second level, known as the high-level trigger, consists of a farm of processors running a version of the full event reconstruction software optimized for fast processing, and reduces the event rate to a few kHz before data storage [47, 48].

Signal events of this analysis are selected online by triggers that require a muon, an electron, a photon, or a large-radius jet to be present in the final state. The photon requirement is added to recover efficiency for events with a very high p_T electron. Different trigger thresholds are used in the different data-taking periods because of changes in the instantaneous luminosity and detector configuration. The high-level trigger selection requires an event to satisfy at least one of the following criteria: presence of a muon with $p_T > 50$ GeV, or an isolated muon with $p_T > 24$ (27) GeV for 2016 and 2018 (2017) data; presence of an isolated electron with $p_T > 27$ (32) GeV for 2016 (2017–2018) data; presence of a photon with $p_T > 175$ (200) GeV for 2016 (2017–2018) data; presence of a large-radius jet with mass >30 GeV and $p_T > 360$, 500 and 400 GeV for 2016, 2017 and 2018 data, respectively.

The combination of the above trigger requirements has an efficiency above 90% for signal events, estimated from simulated samples whose details are described in the following.

JHEP07(2026)041

Simulated background samples are generated at LO with MadGraph5_amc@nlo [49], version 2.6.5, for W+jets events and for events with jets arising exclusively from quantum chromodynamics (QCD) interactions, henceforth referred to as QCD multijet events. The next-to-LO (NLO) generator powheg 2.0 [50–52] is used to simulate top quark-antiquark pair ($\mathrm{t\bar{t}}$) events [53], production of $\mathrm{t\bar{t}}$ events in association with a Higgs boson ($\mathrm{t\bar{t}H}$) [54], and single top quark events produced in the t channel [55] or in association with a W boson [56]. Single top quark events produced in the s channel are generated at NLO with MadGraph5_amc@nlo; this generator and the powheg are interfaced with pythia 8.240 [57] for hadronization and parton shower simulation, with the CP5 underlying event tune [58]. The background processes are initially normalized to their theoretical cross sections, using the highest order available. The cross section for the $\mathrm{t\bar{t}}$ background is computed at next-to-NLO (NNLO) in perturbative QCD using a soft-gluon resummation at next-to-next-to-leading logarithmic precision with the Top++ 2.0 program [59]. For single top quark production, NLO calculations are performed with hathor 2.1 [60]. The W+jets cross section is calculated at LO and corrected with an inclusive K factor to account for NLO electroweak and NNLO QCD corrections [61].

Signal event samples are generated at LO using MadGraph5_amc@nlo interfaced to pythia. We assume a singlet T quark that is produced in association with a bottom quark with suppressed right-handed coupling to SM particles [62]. The generated T quark mass in the samples ranges from 1 to 3 TeV, in steps of 0.1 TeV, and the T quark width Γ is set to 10 GeV, a value much smaller than the experimental resolution, which is of the order of 200–300 GeV. The generated mass of the ϕ boson ranges from 25 to 200 GeV, in steps of 25 GeV. An additional sample is generated with a mass of 250 GeV. All possible leptonic decays of the top quark are simulated for the signal process.

For the interpretation of the results in the case of the tH decay channel, the total cross section is computed at NLO in the narrow-width approximation using the simplified approach from refs. [6, 7], for a singlet T quark assuming a resonance width Γ of 5 or 1% of the mass.

The simulated samples are generated using the NNLO NNPDF 3.1 [63] parton distribution function (PDF) sets.

The generated events are passed through a simulation of the CMS detector based on Geant4 [64, 65]. Additional interactions in the same or adjacent bunch crossings (pileup) are included in the simulation, with their multiplicity distribution adjusted to match that observed in data.

3 Event reconstruction and selection

The primary vertex (PV) is taken to be the vertex corresponding to the hardest scattering in the event, evaluated using tracking information alone, as described in section 9.4.1 of ref. [66]. It must be within 24 cm of the nominal interaction point along the beam axis and within 2 cm in the transverse plane.

A particle-flow (PF) algorithm [67] aims to reconstruct and identify each individual particle in an event, with an optimized combination of information from the various elements of the CMS detector. The energy of photons is obtained from the ECAL measurement. The energy of electrons is determined from a combination of the electron momentum at the PV as determined by the tracker, the energy of the corresponding ECAL cluster, and the energy sum of all bremsstrahlung photons spatially compatible with originating from the electron track. The energy of muons is obtained from the curvature of the corresponding track. The energy of charged hadrons is determined from a combination of their momentum measured in the tracker and the matching ECAL and HCAL energy deposits, corrected for the response function of the calorimeters to hadronic showers. Finally, the energy of neutral hadrons is obtained from the corresponding corrected ECAL and HCAL energies.

Jets are clustered from the PF candidates using the anti-k_{T} algorithm [68, 69] with distance parameters of 0.4 (AK4 jets) and 0.8 (AK8 jets). Jet momentum is determined as the vectorial sum of all particle momenta in the jet, and is found from simulation to be, on average, within 5–10% of the true momentum over the entire spectrum and detector acceptance. Pileup interactions can contribute additional tracks and calorimetric energy depositions, increasing the apparent jet momentum. To mitigate this effect for the AK4 jets, tracks identified to be originating from pileup vertices are discarded and an offset correction is applied to correct for remaining contributions [70]. For the AK8 jets the pileup-per-particle identification algorithm [70, 71] is used to mitigate the effect of pileup at the reconstructed-particle level, making use of local shape information, event pileup properties, and tracking information. A local shape variable is defined, which distinguishes between collinear and soft diffuse distributions of other particles surrounding the particle under consideration. The former is attributed to particles originating from the hard scatter and the latter to particles originating from pileup interactions. Charged particles identified to be originating from pileup vertices are discarded. For each neutral particle, a local shape variable is computed using the surrounding charged particles compatible with the PV within the tracker acceptance ($|\eta| < 2.5$), and using both charged and neutral particles in the region outside of the tracker coverage. The momenta of the neutral particles are then rescaled according to their probability to originate from the PV, deduced from the local shape variable, superseding the need for jet-based pileup corrections [70]. Jet energy corrections are derived from simulation studies so that the average measured energy of jets becomes identical to that of particle level jets. In situ measurements of the momentum balance in dijet, photon+jet, Z+jet, and QCD multijet events are used to determine any residual differences between the jet energy scale in data and in simulation, and appropriate corrections are made [72]. Additional selection criteria are applied to each jet to remove jets dominated by instrumental effects or reconstruction failures [70].

The AK4 jets selected for the analysis must have $p_{\mathrm{T}} > 30\,\mathrm{GeV}$. In order to remove jets originating from pileup, jets with $30 < p_{\mathrm{T}} < 50\,\mathrm{GeV}$ are required to pass the tight working point (WP) of a boosted decision tree (BDT) discriminator [70], which takes jet shapes and kinematic variables as inputs. Signal events are characterized by the presence of a forward jet. At reconstruction level, forward jets are defined as AK4 jets in the region $2.4 < |\eta| < 4.0$. Jets with larger values of $|\eta|$ are not included in the count of forward jets, in order to reduce the contribution from pileup interactions.

Muon (electron) candidates selected for the analysis must have $p_{\mathrm{T}} > 30\,(35)\,\mathrm{GeV}$, $|\eta| < 2.4\,(2.5)$, a transverse distance from the PV less than $0.02\,(0.05)\,\mathrm{cm}$, and satisfy loose identification criteria [73, 74]. Electron candidates are excluded if they are in the ECAL barrel-endcap transition region $1.44 < |\eta| < 1.57$. Selected events must have only one lepton passing the above requirements, in order to reduce contamination from $t\bar{t}$ with two leptons in the final state. Signal events are characterized by a prompt lepton from the top quark decay. In order to discriminate prompt leptons from misidentified ones or leptons from hadronic decay chains, a relative isolation variable $I(\ell)$ [73, 74] is defined as the scalar p_T sum of the hadrons (charged and neutral) and photons in a cone around the lepton direction of size $\Delta R = \sqrt{(\Delta\eta)^2 + (\Delta\phi)^2}$, where $\Delta\eta$ and $\Delta\phi$ are the differences with respect to the lepton direction in η and ϕ. The cone size is 0.4 for muons and 0.3 for electrons. The sum is then corrected for pileup effects and divided by the lepton p_T. A modified relative isolation variable referred to as mini-isolation $I_{\text{mini}}(\ell)$, originally suggested in ref. [75], is also defined, which is optimized for leptons produced in boosted top quark decays by using a p_T-dependent cone size. No isolation requirements are applied on muon and electron candidates used as input for top quark reconstruction; instead, the $I(\ell)$ and $I_{\text{mini}}(\ell)$ variables are employed as input variables to train a top quark tagging algorithm, based on a BDT and described in section 4, to identify true top quark candidates.

The missing transverse momentum vector $\vec{p}_T^{\text{miss}}$ is defined as the negative vector p_T sum of all the PF candidates in an event, and its magnitude is denoted as p_T^{miss} [76]. The $\vec{p}_T^{\text{miss}}$ is modified to account for corrections to the energy scale of the reconstructed jets in the event. Selected events must have $p_T^{\text{miss}} > 25\,\text{GeV}$.

4 Boson and top quark candidate reconstruction

For the reconstruction of the ϕ boson candidates, AK8 jets with $p_T > 500\,\text{GeV}$ and $|\eta| < 2.4$ are used as input. An AK8 jet is tagged as originating from a Lorentz-boosted heavy-boson decay to a bottom quark-antiquark pair (X_{bb} jet) by employing ParticleNet-MD [77], a mass-decorrelated (MD) algorithm. It is based on a dynamic graph convolutional neural network, for identifying two-body hadronic decays of highly boosted particles. The algorithm provides probability-like scores for the AK8 jet to originate from two-prong hadronic decays of the type $X \to b\bar{b}$, $X \to c\bar{c}$, and $X \to q\bar{q}$, or to be a background jet from QCD multijet events. The use of an MD algorithm allows different hypotheses for the ϕ boson mass to be probed without losing signal efficiency. The ParticleNet-MD scores $p(X_{bb})$ and $p(\text{QCD})$ are combined in the XbbVsQCD variable:

$$\text{XbbVsQCD} = \frac{p(X_{bb})}{p(X_{bb}) + p(\text{QCD})}, \tag{4.1}$$

and a threshold on the XbbVsQCD variable is then employed to tag X_{bb} jets.

The mass of an AK8 jet is reconstructed by employing a mass regression technique based on ParticleNet-MD. Events are selected if they have at least one AK8 jet passing a loose WP threshold of the XbbVsQCD tagger with a rejection rate for background jets of 90% and an efficiency for signal jets of 70%, evaluated on jets from simulated QCD multijet and signal events, or if there is at least one AK8 jet with a mass between 60 and 220 GeV.

Top quark candidates are reconstructed from the combination of one lepton candidate ℓ, one AK4 jet with $|\eta| < 2.4$, and the $\vec{p}_T^{\text{miss}}$ of event, following the algorithm described in ref. [78]. Here, the neutrino p_T is assumed to be equal to $\vec{p}_T^{\text{miss}}$ and the longitudinal component of the neutrino momentum is computed by requiring the invariant mass of the lepton-neutrino pair to be equal to the W boson mass [79]. If more than one top quark candidate is reconstructed in the event, all of the candidates are retained for further processing.

In order to suppress combinatorial background, the distance between the lepton and jet directions in the η-ϕ plane, $\Delta R_{\ell j}$, must be less than 2. If $\Delta R_{\ell j} < 0.4$, the lepton is likely to overlap with the jet, and the top quark candidate is said to be in the merged configuration. In this case, the lepton four-momentum is subtracted from the jet four-momentum before computing the top quark candidate four-momentum. Otherwise, if $0.4 < \Delta R_{\ell j} < 2.0$, the top quark candidate is said to be in the resolved configuration. A deep neural network based tagger, DeepJet [80–82], is used to identify AK4 jets stemming from the hadronization of b quarks, by exploiting information from the tracks, neutral particles, and the secondary vertices within the jet. The output of the b tagger is employed as one of the input variables of the top quark tagging algorithm, based on a BDT, which is described below.

Simulated samples are used to train a machine learning algorithm to identify top quark decays. In these samples, generator information at parton level is employed to perform an angular matching of the top quark decay products with the leptons and jets reconstructed in the event. A successful matching of both the lepton and the jet defines what we henceforth refer to as a true top quark candidate ($\mathrm{t_{true}}$). The properties of $\mathrm{t_{true}}$ candidates with respect to the combinatorial background have been studied. Background candidates where neither the lepton nor the AK4 jet originate from the decay of a top quark, which are typical of QCD multijet events ($\mathrm{t_{QCD}}$ candidates), are distinguished from all other types of background ($\mathrm{t_{oth}}$ candidates). The latter category includes, for instance, combinatorial candidates in genuine top quark events, in which the lepton and the AK4 jet do not both originate from the decay of the same top quark, which are typical of $\mathrm{t\bar{t}}$ background events. A multiclass BDT algorithm, making use of the XGBoost library [83], is trained to distinguish $\mathrm{t_{true}}$ from $\mathrm{t_{QCD}}$ and $\mathrm{t_{oth}}$ candidates. Separate BDTs are trained for the merged or resolved configuration of the top quark candidate, for each lepton flavor (muon or electron), and for a top quark candidate with transverse momentum p_{T} above 500 GeV (high-p_{T} candidate) or below (low-p_{T} candidate).

In total, eight different trainings have been performed, each using a different set of input variables, which are related to the top quark candidate as well as to the associated lepton and AK4 jet. The input variables are:

- the p_{T} of the jet ($p_{\mathrm{T}}(j)$);
- the mass of the jet ($M(j)$);
- the value of the DeepJet b tagger score for the jet (b tag(j));
- the p_{T} of the lepton ($p_{\mathrm{T}}(\ell)$);
- the distance of closest approach of the lepton with respect to the PV in the transverse plane ($d_{xy}(\ell)$) and its uncertainty ($\sigma_{xy}(\ell)$);
- the distance of closest approach of the lepton with respect to the PV along the longitudinal direction ($d_z(\ell)$) and its uncertainty ($\sigma_z(\ell)$);
- the lepton isolation ($I(\ell)$) and mini-isolation ($I_{\mathrm{mini}}(\ell)$);

- the ratio of the lepton to jet p_{T};
- the separation $\Delta R_{\ell j}$ between the lepton and jet directions in the η-ϕ plane;
- the component of the lepton momentum orthogonal to the jet axis ($p_{\mathrm{T}}^{\mathrm{rel}}(\ell)$);
- the cosine of the angle between the lepton and the jet in the top quark candidate reference frame ($\cos\theta_{\ell j}$);
- the invariant mass of the lepton+jet system ($M(\ell j)$);
- the p_{T} of the lepton+jet system ($p_{\mathrm{T}}(\ell j)$);
- the invariant mass of the top quark candidate ($M(\ell\nu j)$);
- the transverse mass of the top quark candidate ($M_{\mathrm{T}}(\ell\nu j)$);
- the p_{T} of the top quark candidate ($p_{\mathrm{T}}(\ell\nu j)$).

The set of variables used in each of the trainings is reported in table 1.

For a given top quark candidate, the BDT classifier provides three probability-like scores: $p(\mathrm{t_{true}})$, $p(\mathrm{t_{QCD}})$, and $p(\mathrm{t_{oth}})$. Two variables, TopVsQCD and TopVsOther, are defined as follows in order to discriminate $\mathrm{t_{true}}$ candidates from $\mathrm{t_{QCD}}$ and $\mathrm{t_{oth}}$ background candidates, respectively:

$$\mathrm{TopVsQCD} = \frac{p(\mathrm{t_{true}})}{p(\mathrm{t_{true}}) + p(\mathrm{t_{QCD}})}; \tag{4.2}$$

$$\mathrm{TopVsOther} = \frac{p(\mathrm{t_{true}})}{p(\mathrm{t_{true}}) + p(\mathrm{t_{oth}})}. \tag{4.3}$$

The discrimination powers of the TopVsQCD and TopVsOther top quark tagging variables are illustrated in figure 2, showing their respective receiver operating characteristic curves. A comparison with a cut-based selection is also shown; this selection requires the lepton to be isolated and applies a b tagging score threshold with a background efficiency of 1%. The top quark candidate for the cut-based approach is then chosen as the one with the lowest difference in mass with respect to the nominal top quark mass value taken from ref. [79]. For a background misidentification rate of about 6%, the selection based on the BDT gives a relative improvement on the true top quark candidate identification efficiency of about 30%.

Top quark candidates are required to be above a threshold of the TopVsQCD score, with a signal efficiency of 99%, and to satisfy the loose or the tight WP requirement of the TopVsOther variable, which respectively correspond to a background rejection rate of 90 and 99%. The signal efficiency and background misidentification rate are evaluated on top quark candidates with an associated muon, with $p_{\mathrm{T}} > 500\,\mathrm{GeV}$ and in the merged configuration in simulated $\mathrm{t\bar{t}}$ events.

Events are selected if at least one top quark candidate passes the loose WP of the TopVsOther tagger. Events with no loosely tagged top quark candidates are still selected if the lepton satisfies tight identification requirements (referred to in the following as "tight lepton"); these events are employed to calibrate the $\mathrm{X_{bb}}$ tagging as described in section 6.

	Electron channel				Muon channel			
	Resolved		Merged		Resolved		Merged	
	Low-p_{T}	High-p_{T}	Low-p_{T}	High-p_{T}	Low-p_{T}	High-p_{T}	Low-p_{T}	High-p_{T}
$M(j)$	✓	✓	✓	✓	✓	✓	✓	✓
$p_{\mathrm{T}}(j)$	✓	✓	✓		✓			
b tag(j)	✓	✓	✓	✓	✓	✓	✓	✓
$p_{\mathrm{T}}(\ell)$	✓							
$d_{xy}(\ell)$	✓	✓	✓	✓	✓	✓	✓	✓
$\sigma_{xy}(\ell)$	✓				✓			
$d_z(\ell)$	✓	✓	✓	✓	✓		✓	✓
$\sigma_z(\ell)$	✓				✓			
$I(\ell)$	✓	✓	✓	✓	✓	✓	✓	✓
$I_{\mathrm{mini}}(\ell)$	✓	✓	✓	✓	✓	✓	✓	✓
$p_{\mathrm{T}}(\ell)/p_{\mathrm{T}}(j)$	✓		✓	✓			✓	
$M(\ell\nu j)$	✓	✓	✓	✓	✓	✓	✓	✓
$p_{\mathrm{T}}(\ell\nu j)$	✓		✓		✓		✓	✓
$M(\ell j)$	✓	✓			✓	✓		
$p_{\mathrm{T}}(\ell j)$	✓							
$M_{\mathrm{T}}(\ell\nu j)$	✓	✓	✓	✓		✓		✓
$p_{\mathrm{T}}^{\mathrm{rel}}(\ell)$	✓	✓	✓	✓		✓	✓	✓
$\cos\theta_{\ell j}$	✓		✓		✓			✓
$\Delta R_{\ell j}$	✓		✓	✓	✓	✓		

Table 1. List of the variables employed for each of the eight trainings of the multiclass BDT algorithm for top quark candidate identification. The trainings are different for each lepton channel, for the merged or resolved configuration of the top quark candidate, and for the p_{T} range of the top quark candidate with a threshold of 500 GeV.

5 Event categorization

Selected events are assigned to mutually exclusive categories, which are used for signal extraction or as background control regions (CRs). Where there are multiple reconstructed top quark or ϕ boson candidates in an event, a procedure is defined to select only one of them, as described below.

Three exclusive event categories are defined, based on the tagging quality of the reconstructed top quark candidates. A block diagram illustrating the workflow to assign an event to one of these three top quark tagging categories is shown in figure 3 (left). An event is assigned to the TopT category if there is at least one top quark candidate passing the tight WP requirement of the TopVsOther tagger. Events with no top quark candidates passing the above selection, but with at least one candidate passing the loose WP of the TopVsOther tagger, are assigned to the TopL category.

JHEP07(2026)041

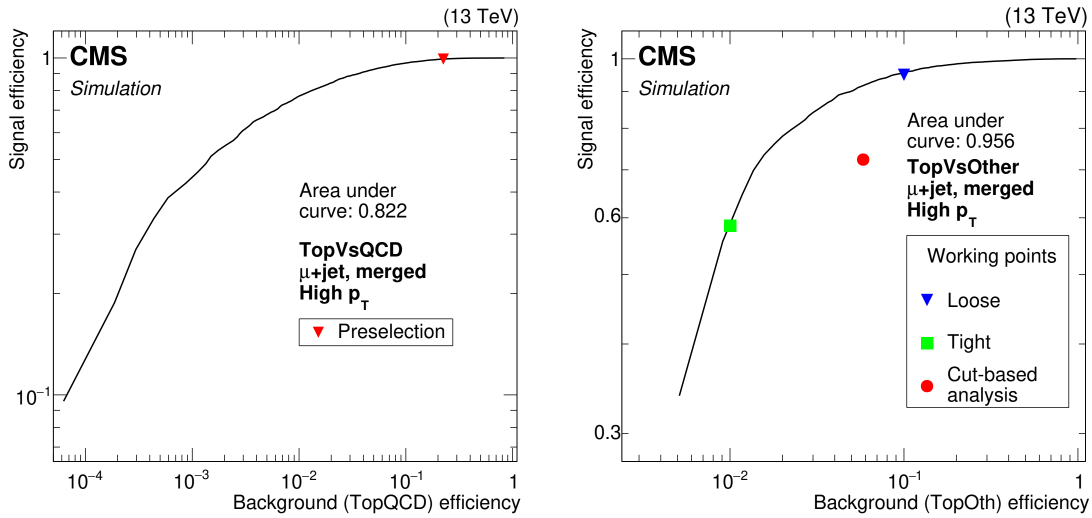

Figure 2. The receiver operating characteristic curve for the TopVsQCD (left) and TopVsOther (right) top quark taggers. The signal efficiency and background misidentification rate are evaluated on top quark candidates with an associated muon, with $p_{\mathrm{T}} > 500\,\mathrm{GeV}$ and in the merged configuration in simulated $\mathrm{t\bar{t}}$ events. The red triangle in the left plot corresponds to the requirement on the TopVsQCD variable providing a signal efficiency of 99%; the blue triangle and the green square in the right plot correspond to the loose and tight WP of the TopVsOther tagger, respectively. A comparison with a cut-based selection (red point) is also shown in the TopVsOther case.

If there are multiple top quark candidates passing the tight (loose) WP in the TopT (TopL) category, they are ordered as follows, and the highest in the order is selected as the top quark candidate in the event. The highest priority is given to a high-p_{T} top quark candidate in the merged configuration, then to a low-p_{T} (then high-p_{T}) candidate in the resolved configuration, and lastly to a low-p_{T} candidate in the merged configuration. Top quark candidates with the same priority are ordered by descending values of the TopVsOther tagger output.

Events not assigned to any of the above categories are required to contain one tight lepton and assigned to the LeptonTight (LepT) category.

In order to further reduce the $\mathrm{t\bar{t}}$ and QCD multijet background, the events must also pass the following requirements:

- for events in the TopT or TopL category, the top quark candidate must have TopVsQCD > 0.6;
- to exploit the fact that the top quark and ϕ boson are produced mainly back-to-back in the CMS rest frame, there must be at least one AK8 jet that is separated from the top quark candidate by $\Delta R > 1.2$, from the AK4 jet of the top quark candidate by $\Delta R > 1.2$, and from the lepton of the top quark candidate by $\Delta R > 0.8$;
- for events in the LepT category, there must be at least one AK8 jet that is separated from the tight lepton of the event by $\Delta R > 0.8$.

The AK8 jet with the largest value of the XbbVsQCD tagger, selected among the ones passing the above ΔR requirements, is chosen as the ϕ boson candidate of the event and,

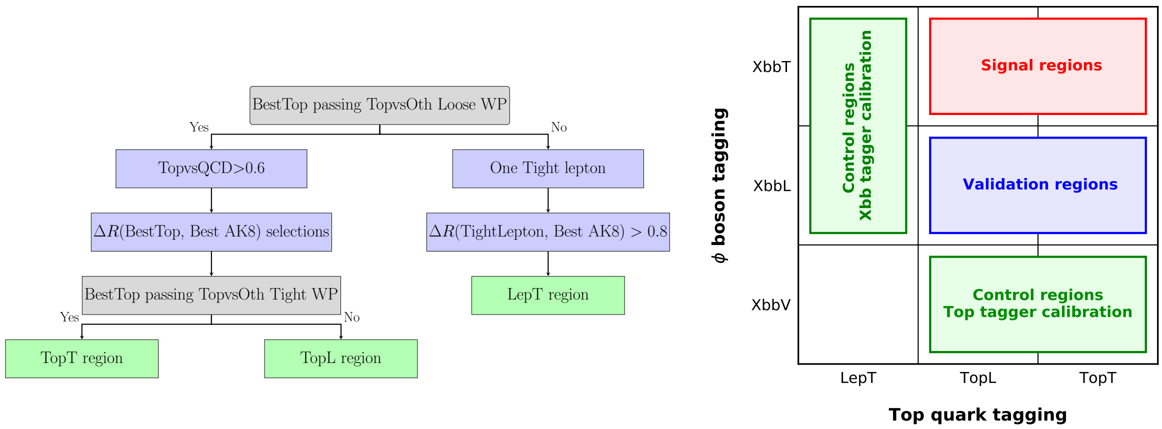

Figure 3. Left: block diagram showing the event classification based on top quark tagging. Right: schematic view of the signal, validation, and control regions defined in the analysis. The label BestTop (Best AK8) refers to the top quark candidate (AK8 jet) with the highest value of the TopVsOther (XbbVsQCD) tagger. The labels TopT (Top Tight) and TopL (Top Loose) refer to events where there is a top quark passing a tight working point for the TopVsOther tagger with a background rejection of 99%, or a loose working point with a background rejection of 90% while vetoing the tight working point to ensure statistical independence of the categories. The label LepT refers to events that are neither in the TopT or TopL categories, but where a top quark candidate is built via a lepton and b-jet pair. The XbbT, XbbL, and XbbV labels refer to the fact that the largest score of the XbbVsQCD tagger evaluated on AK8 jets selected in the event is in the XbbVsQCD range of (>0.98), (0.80–0.98), or (<0.80), respectively. Additionally, for the event to be included in the XbbV category, the mass of the jet with the largest score is required to be in the 60–220 GeV range.

depending on the value of the tagger output, the event is assigned to one of three exclusive categories as follows: if XbbVsQCD > 0.98 or $0.80 <$ XbbVsQCD < 0.98, the event is assigned to the XbbTight (XbbT) or XbbLoose (XbbL) category, respectively; if XbbVsQCD < 0.80 and the AK8 jet mass is in the 60–220 GeV range, the event is assigned to the XbbVeto (XbbV) category; otherwise the event is discarded.

Nine independent event regions are thus defined, based on all the possible combinations of the three top quark tagging categories (TopT, TopL, LepT) and the three X_{bb} tagging categories (XbbT, XbbL, XbbV) the event may belong to, as shown in figure 3 (right).

Events in the (TopT, XbbT) and (TopL, XbbT) regions, which have the largest signal-to-background ratio across all regions, are used for signal extraction (signal regions, SRs). Events in the signal-depleted regions (TopT, XbbL) and (TopL, XbbL) are employed as validation regions (VRs) to verify that good agreement is found between data and background prediction, and to constrain the background in the final fit. The events in each of these regions are further divided in subcategories, depending on the flavor of the lepton (muon or electron) of the top quark candidate and the presence or absence of at least one forward jet, to exploit the presence in signal events of high-pt quarks produced at low angle with respect to the beam axis.

For each event belonging to the SRs or VRs, a T quark candidate is reconstructed by summing together the four-momenta of the reconstructed top quark candidate and of the AK8 jet chosen as the ϕ boson candidate. The distribution of the invariant mass of the T quark candidate $M_{\ell\nu bJ}$ is then used in the final fit for signal extraction.

The regions (TopT, XbbV) and (TopL, XbbV), as well as the regions (LepT, XbbT) and (LepT, XbbL), are employed as CRs for top quark tagging and $\mathrm{X_{bb}}$ tagging calibration, respectively. The signal-to-background ratio in the CRs is lower by a factor of 15–30 compared to the SRs.

6 Background estimation

After the event selection, the major sources of background in the SRs are mainly $\mathrm{t\bar{t}}$ events, followed by single top quark events, and, to a lesser extent, $\mathrm{t\bar{t}H}$, QCD multijet and W+jets events. Other sources, such as diboson processes and top quarks produced in association with vector bosons, are found to be negligible both in the SRs and CRs.

The event rates and distribution shapes used as input to the final fit for signal extraction are derived from simulated events. Data-to-simulation correction factors are applied to simulated events in order to correct small discrepancies between data and simulation in the trigger and reconstruction efficiencies, and for the lack of higher-orders corrections in the simulation.

A relevant aspect of the analysis is the usage of top quark and $\mathrm{X_{bb}}$ tagging to identify the top quark and ϕ boson candidates, respectively. Data-to-simulation correction factors for the tagger efficiency and mistag rate are determined from the CRs, and applied to simulated signal and background events. The corrections correspond to variations from the predicted efficiency or mistag rate in the range between 5 and 15%.

Events in the (TopT, XbbV) and (TopL, XbbV) regions have a top quark candidate satisfying top quark tagging criteria. They are employed to calibrate the top quark tagger efficiency and mistag rate by means of a background-only fit to the b tag(j) distribution of the AK4 jet associated to the top quark candidate. In the fit, the templates of the background distributions are divided in three components, according to the type of the reconstructed top quark candidate ($\mathrm{t_{true}}$, $\mathrm{t_{QCD}}$, or $\mathrm{t_{oth}}$), as inferred from generator-level information, and the top quark tagging correction factors are determined from the fitted yields of these components. The fit takes into account the correlation of event yields in the TopL and TopT categories, since a change in the top quark tagging efficiency may cause migration of events from one category to the other. Different correction factors are determined for events in the muon and electron channels. All the systematic effects, which are described in section 7, are included in the fit by means of nuisance parameters.

Background events in the (LepT, XbbT) and (LepT, XbbL) regions have an AK8 jet misidentified as a ϕ boson candidate and are employed to calibrate the mistag rate of the $\mathrm{X_{bb}}$ tagger. Correction factors are determined from the fitted event yields of the background components in a fit to the distribution of reconstructed mass $M_{\mathrm{X_{bb}}}$ of the $\mathrm{X_{bb}}$ jet selected as the ϕ boson candidate. Only events with $M_{\mathrm{X_{bb}}} > 110\,\mathrm{GeV}$ are considered for the fit, since in this mass range the background compositions of the CRs agrees with those of the SRs and VRs. The templates of the background distributions are divided in two components: resonant background events from all-hadronic top quark decays and nonresonant background events. The fit takes into account the correlation of event yields in the XbbL and XbbT categories, since a change in the $\mathrm{X_{bb}}$ tagging efficiency may cause migration of events from one category to the other. All the systematic effects, which are described in section 7, are

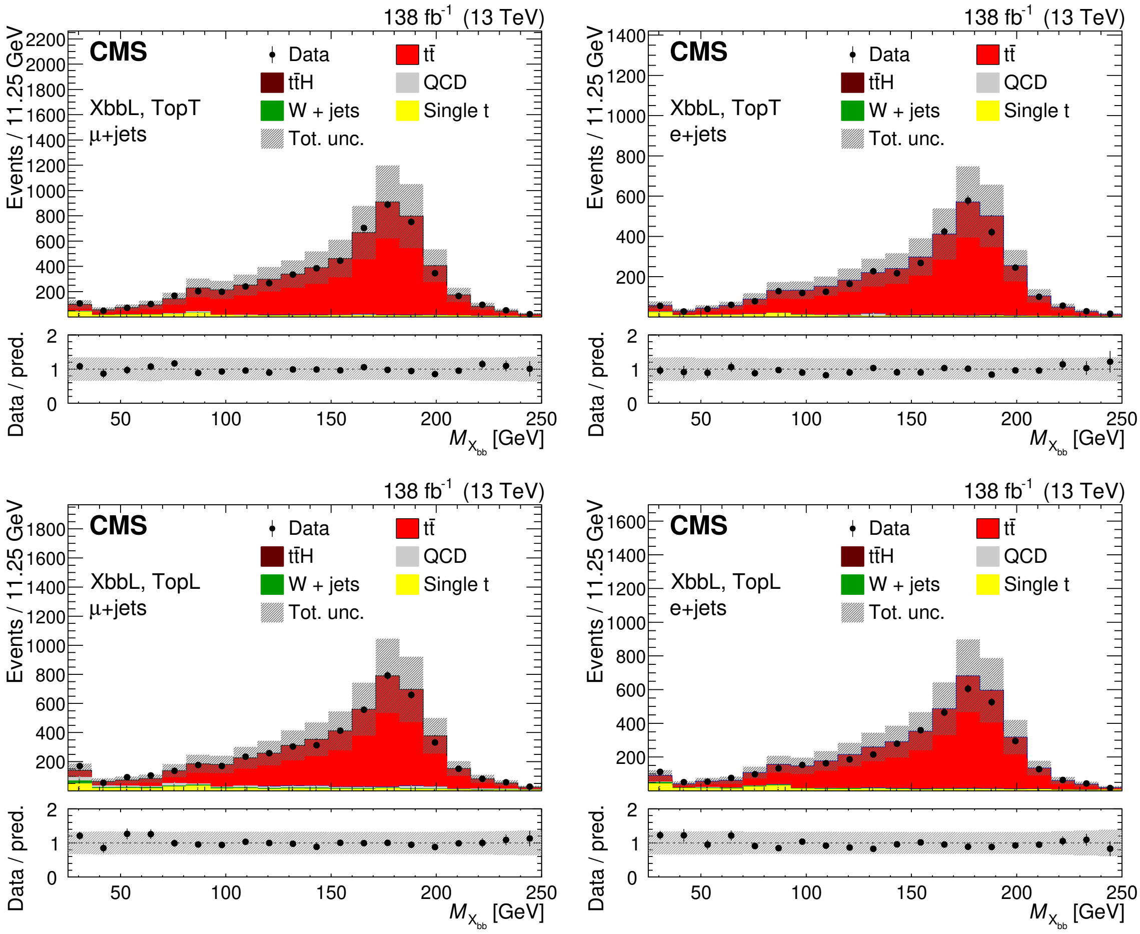

Figure 4. Distribution of the $M_{\mathrm{X_{bb}}}$ mass of the AK8 jet selected as the ϕ boson candidate for data and simulated background events in the (TopT, XbbL) (upper), in the (TopL, XbbL) (lower) VRs, for the muon (left) and electron channels (right). The distributions are shown before the final fit for signal extraction.

included in the fit by means of nuisance parameters. As a proof that the mistag correction factors are independent of $M_{\mathrm{X_{bb}}}$, figure 4 shows the $M_{\mathrm{X_{bb}}}$ distribution for events in the VRs (TopT, XbbL) and (TopL, XbbL), with all the correction factors applied and before the final fit for signal extraction.

The efficiency of the $\mathrm{X_{bb}}$ tagger to identify correctly an $\mathrm{X_{bb}}$ jet is calibrated using data with energetic gluons splitting to bottom quarks [84]. Data-to-simulation correction factors are derived in bins of the AK8 jet p_{T} and applied to simulated signal events and $\mathrm{t\bar{t}H}$ background events.

7 Systematic effects and uncertainties

Systematic uncertainties, both of theoretical and experimental origin, affect the event rate of the background and signal predictions, the shape of $M_{\ell\nu\mathrm{bJ}}$ invariant mass distribution, or both. Depending on the source, the uncertainties are treated as fully correlated or fully uncorrelated among the different data-taking periods, or decomposed into a correlated and an uncorrelated component.

Most of the uncertainties are related to the corrections that are applied to simulated events in order to account for the known discrepancies with data. In this case, and for each systematic correction, modified signal and background distributions are obtained by shifting the nominal value of the correction up and down by one standard deviation. A summary of the systematic uncertainties is reported in table 2.

The integrated luminosity of the entire 2016–2018 dataset has an uncertainty of 1.6% [85–87], which applies to the overall event rates of all simulated processes.

The uncertainty associated with the mismodeling of pileup is evaluated by varying the total inelastic pp cross section used to compute the pileup distribution in data by $\pm4.6\%$ [88].

Lepton and jet trigger efficiencies are measured in data and simulated samples as a function of lepton p_T and η, and AK8 jet p_T and mass. Data-to-simulation scale factors (SF) are then obtained and applied to simulated events.

During the 2016–2017 data taking, a gradual shift in the timing of the inputs of the ECAL L1 trigger in the region $|\eta| > 2.0$ caused a specific trigger inefficiency. For events containing a jet with $p_\mathrm{T} \gtrsim 100\,\mathrm{GeV}$ in the region $2.5 < |\eta| < 3.0$, the efficiency loss is approximately 10–20%, depending on p_T, η, and data-taking period [46]. Correction factors are computed from data and applied to the acceptance evaluated from simulation.

Differences between data and simulation in the efficiency of lepton reconstruction and identification (ID) are corrected by applying SFs, which are functions of lepton p_T and η, to simulated events.

The SFs are also applied to simulated events in order to reproduce the efficiency of the pileup BDT discriminator cut applied to AK4 jets with $30 < p_\mathrm{T} < 50\,\mathrm{GeV}$ to remove jets originating from pileup.

Systematic effects due to differences in the jet energy scale between data and simulation are evaluated by varying the jet four-momenta in simulated events, according to the p_T and η-dependent uncertainties in the jet energy scale. Similarly, in order to evaluate systematic effects due to differences in the jet energy resolution between data and simulation, a smearing is applied to simulated events by increasing or decreasing the jet resolutions by their uncertainties [72]. The variations in jet four-momenta are also propagated to the $\vec{p}_\mathrm{T}^\mathrm{miss}$.

Correction factors for the top quark and $\mathrm{X_{bb}}$ tagging are derived from fits to data in the CRs, as described in section 6, and by using data events with energetic gluons splitting to bottom quarks [84]. The uncertainties in the correction factors are taken as the systematic uncertainties in the top quark and $\mathrm{X_{bb}}$ tagging.

The uncertainties from the choice of the PDFs are evaluated by reweighting the simulated signal and background events using the NNPDF 3.1 Hessian uncertainties [89].

Source	Rate/shape	Correlation	Impact ($m_T = 1.8\,\text{TeV}$) [%]
X_{bb} tagging	shape	correlated + uncorrelated	20–90
Top quark tagging	shape	correlated + uncorrelated	10–40
Simulated samples size	shape	uncorrelated	40–60
μ_R, μ_F	shape	correlated	10–20
Parton distribution functions	shape	correlated	5–8
Top quark p_T reweighting	shape	correlated	<1
Pileup jet identification	shape	correlated	5–15
ECAL L1 trigger inefficiency	shape	correlated	4–5
Jet energy scale	shape	uncorrelated	3–5
Jet energy resolution	shape	uncorrelated	3–5
Jet pileup identification	shape	correlated	<1
Trigger	shape	uncorrelated	2–5
Lepton reconstruction and ID	shape	correlated + uncorrelated	2–5
Integrated luminosity	rate	correlated	1–2

Table 2. List of systematic uncertainties, showing whether a source modifies the event rate or the distribution shape, and whether the effect is correlated or uncorrelated across the years of data taking. All the listed sources affect both signal and background processes. The relative impact on the postfit signal strength is shown for a representative set of signals with a T mass (m_T) hypothesis of 1.8 TeV and varying the mass of ϕ boson.

Simulated $t\bar{t}$ events are corrected by applying event weights derived from the ratio of top quark p_T, measured in data at parton level, and NNLO predictions [90]. An uncertainty of $\pm 50\%$ of the applied correction is assigned to this event reweighting.

The choice of the factorization and renormalization scales, μ_F and μ_R, affects both the cross section and the acceptance of each background. The uncertainties are estimated separately for each background by halving or doubling each of the scales, compared to the nominal values used in simulation.

The statistical uncertainty due to the limited size of simulated event samples is evaluated for each bin with the Barlow–Beeston "lite" method [91, 92]. The impact of this systematic effect on the result of the fit is large in the high-mass bins of the $M_{\ell\nu bJ}$ distribution, in particular above 1.5 TeV, due to the fall-off of standard model background processes. This systematic uncertainty is also not reduced by the simultaneous fit to VR and SR, since it is uncorrelated across bins and regions.

8 Results

The signal extraction procedure is based on a simultaneous maximum likelihood fit to the invariant mass distribution of the T quark candidates $M_{\ell\nu bJ}$ in the (TopT, XbbT) and (TopL, XbbT) SRs, and (TopT, XbbL) and (TopL, XbbL) VRs. The events are divided into 16 categories defined according to the specific SR or VR, the lepton channel, and the presence or absence of at least one forward jet. Systematic uncertainties are treated in the fit as nuisance parameters, assumed to be described by a log-normal probability density function

JHEP07(2026)041

m_ϕ [GeV]	$M_{X_{bb}}$ requirement [GeV]
25	$[20, 34]$
50	$[41, 73]$
75	$[60, 100]$
100	$[78, 130]$
125	$[97, 160]$
150	$[120, 190]$
175	$[140, 210]$
200	$[160, 230]$
250	>190

Table 3. Requirement on the reconstructed $M_{X_{bb}}$ mass of the ϕ boson candidate, as a function of the m_ϕ boson mass hypothesis being tested. The $M_{X_{bb}}$ mass must fall within the specified interval.

for those that affect the rate, or a Gaussian probability density function for those that also affect the shape of the distributions.

Events used as input to the fit must satisfy a requirement on the reconstructed $M_{X_{bb}}$ mass of the ϕ boson candidate, which is defined such that it selects 95% of signal events and depends on the ϕ boson mass (m_ϕ) hypothesis being tested, as shown in table 3. The requirement is asymmetric with respect to the m_ϕ value, because of the asymmetric tails of the $M_{X_{bb}}$ mass distribution, with the left tail becoming broader as m_ϕ increases. In the hypothesis of the SM Higgs boson ($T \to tH$ decay), the requirement $110 < M_{X_{bb}} < 140\,\text{GeV}$ is imposed, to optimize the analysis sensitivity. Figure 5 shows the fitted $M_{\ell\nu bJ}$ distributions of the T quark candidates for events in the SRs (TopT, XbbT), and (TopL, XbbT), with at least one forward jet, and passing the $M_{X_{bb}}$ selection of the $T \to tH$ decay analysis.

The following results have been determined using COMBINE [93], the CMS statistical analysis tool, which is based on the ROOFIT [94] and ROOSTATS [95] frameworks.

No evidence of a statistically significant signal is found from the fit to the data. An upper limit at 95% confidence level (CL) is set on the product of the production cross section and $T \to t\phi \to b\ell\nu b\bar{b}$ branching fraction as a function of the T quark mass (m_T) and m_ϕ hypotheses, as shown in figure 6. The limits are determined using the CL_s method [96–99], taking the profile likelihood ratio as the test statistic with the asymptotic limit approximation. For a fixed m_T, the upper limit tends to increase with m_ϕ, because the looser requirement applied on $M_{X_{bb}}$ increases the amount of the selected background.

Figures 7 and 8 show the 95% CL upper limits on the single T quark product of cross section and $T \to t\phi \to b\ell\nu b\bar{b}$ branching fraction as a function of m_T for fixed values of m_ϕ in the range $[25, 250]$ GeV. For $m_\phi = 25$ (250) GeV, values greater than 2.3 to 0.1 (14.7 to 0.3) fb are excluded at 95% CL for m_T between 1.0 and 3.0 (1.3 and 3.0) TeV.

In the case of the $T \to tH$ decay analysis, the 95% CL upper limits on the product of the production cross section and $T \to tH$ branching fraction as a function of m_T are shown in figure 9. Values greater than 100 to 1.0 fb are excluded at 95% CL for m_T between 1 and

JHEP07(2026)041

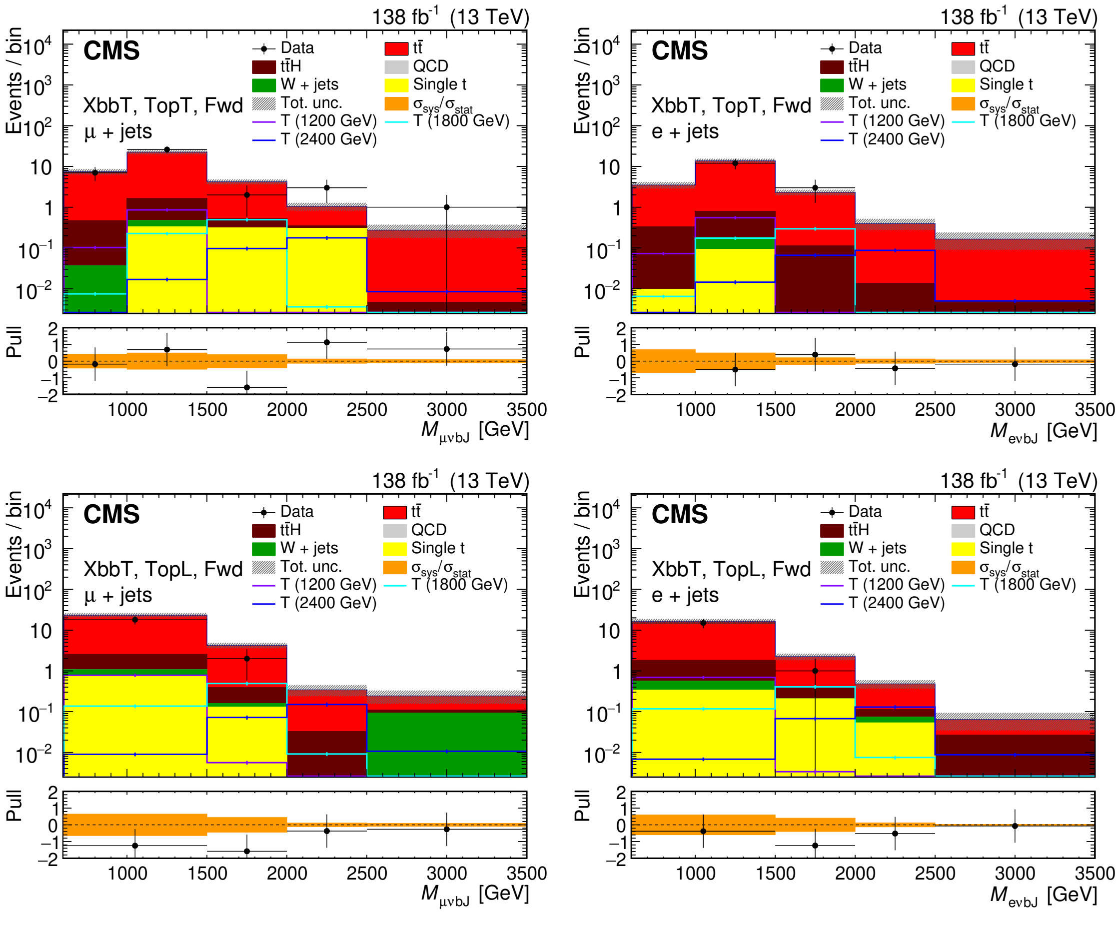

Figure 5. Invariant mass distribution of the T quark candidates selected in the T → tH channel, for events with at least one forward jet and in the SRs for (TopT, XbbT) (upper) and (TopL, XbbT) (lower). For these events, the reconstructed mass of the Higgs boson candidate is required to be between 110 and 140 GeV. Distributions are shown for events in the muon (left) and electron (right) channel. The first (last) bin of each distribution also includes underflow (overflow) events. Background distributions are normalized to the results of the background-only fit, while signal distributions are overlaid, normalized to the expected cross section computed at NLO for a singlet T quark with a resonance width Γ of 1% of the mass. The lower panels show the difference between the number of events in data and that expected from the background-only fit, normalized to the statistical uncertainty of the data. When no events are observed in data, the Poissonian upper limit at 68% CL is used for the calculation of the pull. The orange band represents the systematic uncertainties, also normalized to the statistical uncertainty of the data.

3 TeV. The limits are compared with theoretical expectations assuming a singlet T quark with a resonance width Γ of 5 or 1% of the mass. As a result of a reconstruction strategy optimized for large Lorentz boost of the T quark decay products, the analysis is particularly sensitive to signal production for large m_T values. In the singlet scenario, this analysis improves on all previous searches performed in CMS [9, 31, 32, 34, 41] for m_T values of 1.3 TeV and above, and it provides the strongest limits to date for $m_T > 2$ TeV. Nevertheless, the analysis sensitivity is also comparable with other searches in the range $1.1 < m_T < 1.3$ TeV and, for a

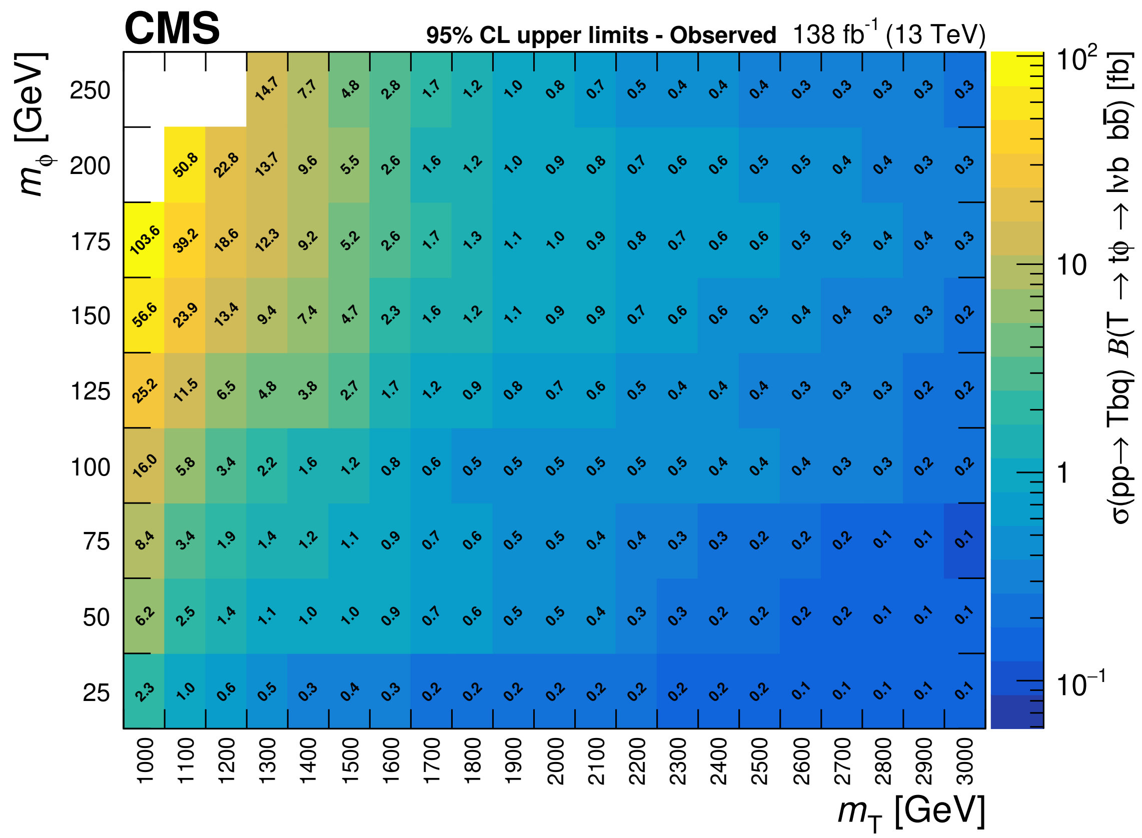

Figure 6. Observed 95% CL upper limits on the single T quark product of cross section and branching ratio for the $\mathrm{T} \to \mathrm{t}\phi \to \mathrm{b}\ell\nu\mathrm{b}\overline{\mathrm{b}}$ channel, as a function of m_{T} and m_{ϕ} masses.

Γ/m_{T} ratio of 5%, it is near the level of excluding m_{T} around 1.2 TeV. As a comparison, the T quark search exploiting final states with one lepton and multiple jets reported by the ATLAS Collaboration [33], and targeting the tH and tZ decay channels, excluded T quark masses, in the singlet scenario and for a Γ/m_{T} ratio of 5%, from 1 to almost 1.2 TeV at 95% CL.

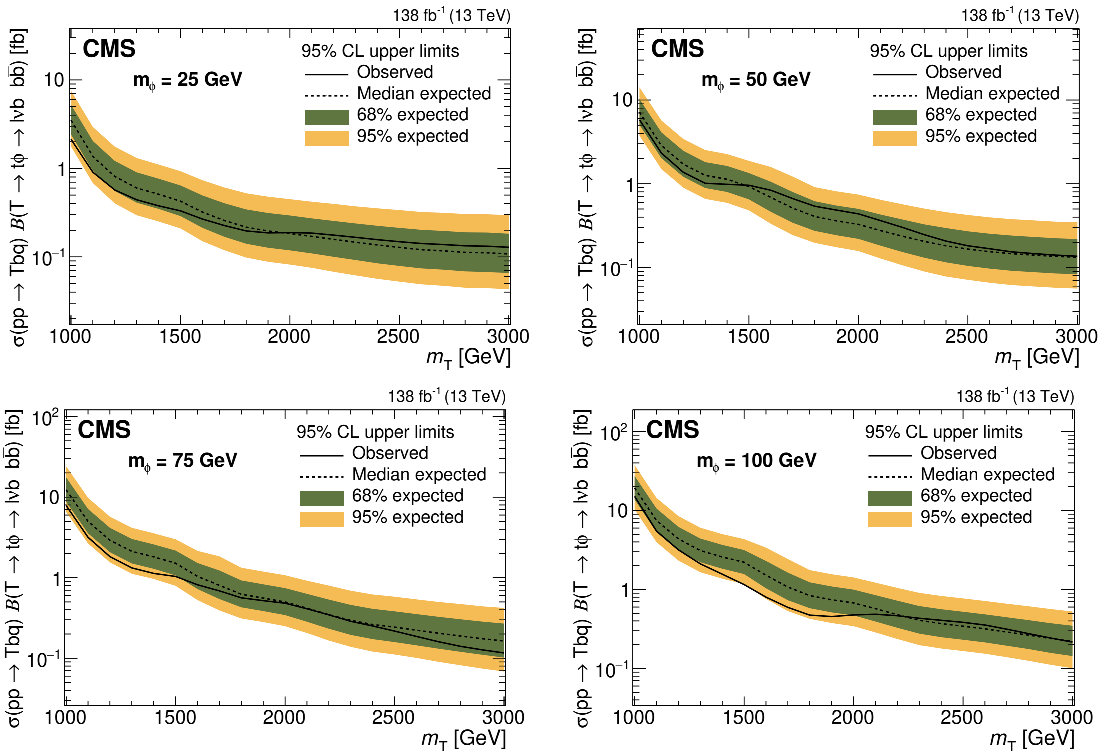

Figure 7. Observed (solid lines) and expected (dashed lines) 95% CL upper limits on the single T quark product of cross section and branching ratio for the $\mathrm{T} \to \mathrm{t}\phi \to \mathrm{b}\ell\nu\mathrm{b}\bar{\mathrm{b}}$ channel as a function of m_{T}, for fixed values of m_ϕ, from 25 up to 100 GeV. The inner (green) and outer (yellow) bands represent the regions containing 68 and 95%, respectively, of the limit values expected under the background-only hypothesis.

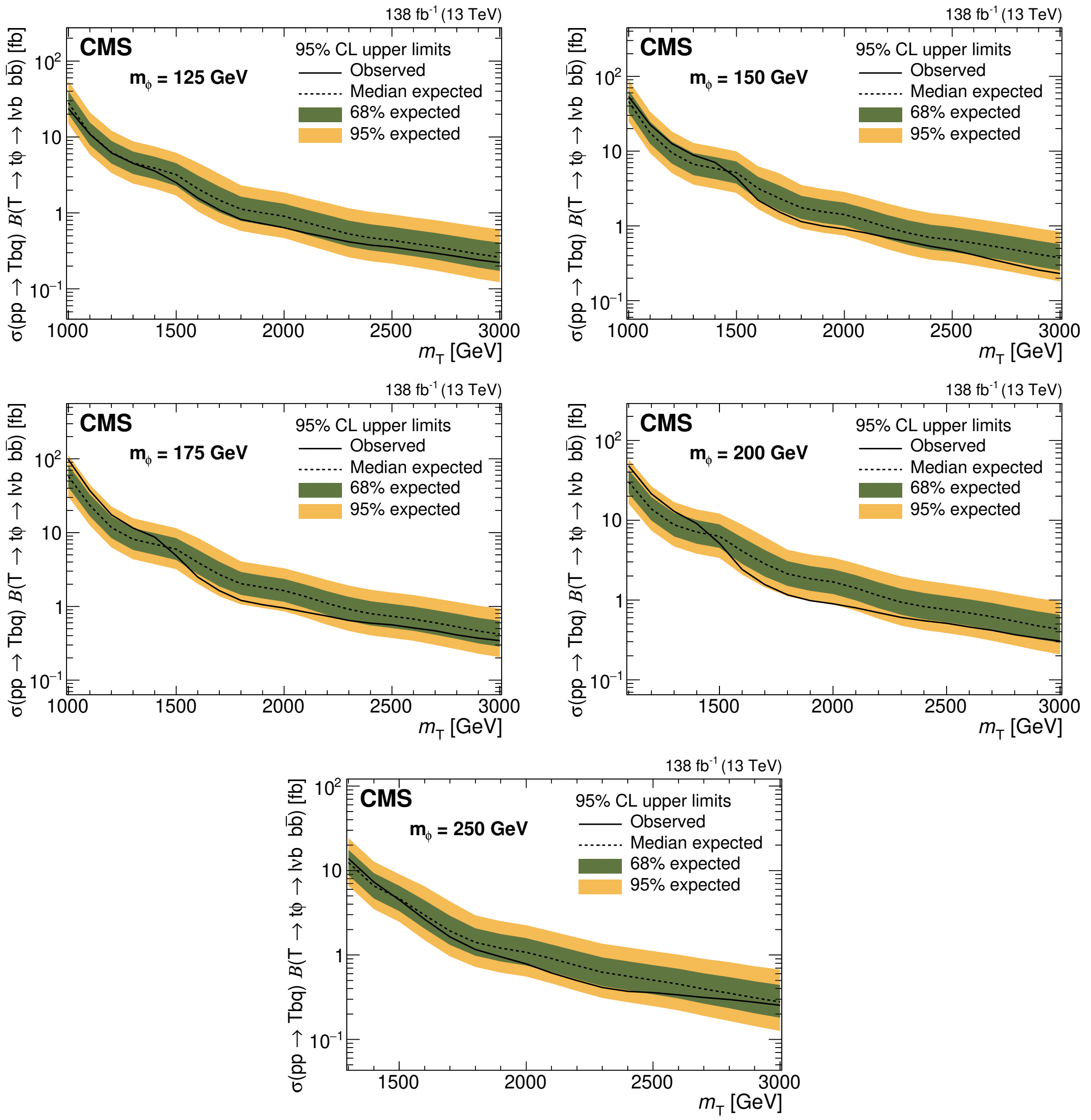

Figure 8. Observed (solid lines) and expected (dashed lines) 95% CL upper limits on the single T quark product of cross section and branching ratio for the $T \to t\phi \to b\ell\nu b\bar{b}$ channel as a function of m_T, for fixed values of m_ϕ, from 125 up to 250 GeV. The inner (green) and outer (yellow) bands represent the regions containing 68 and 95%, respectively, of the limit values expected under the background-only hypothesis.

JHEP07(2026)041

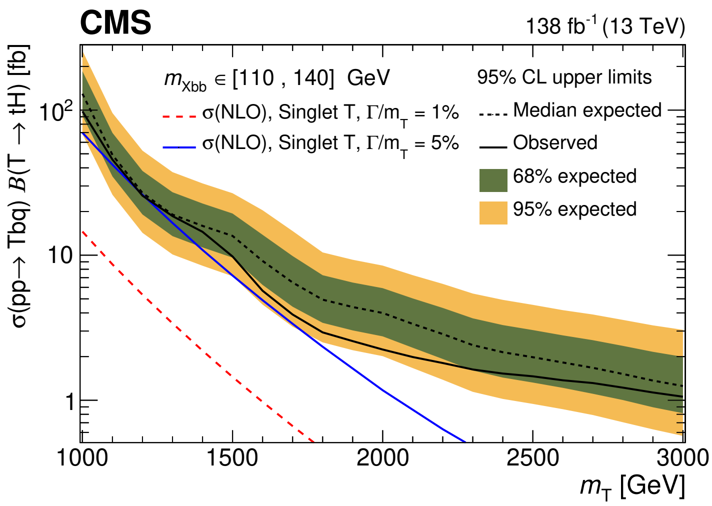

Figure 9. Observed (solid black line) and expected (dashed line) 95% CL upper limit on the single T quark production cross section times branching fraction for the $\mathrm{T} \to \mathrm{tH}$ channel as a function of the m_{T} mass. The inner (green) and outer (yellow) bands represent the region containing 68 and 95%, respectively, of the limit values expected under the background-only hypothesis. The solid blue (dashed red) curve shows the theoretical expectation at NLO for a singlet T quark assuming a narrow resonance with width 5% (1%) of the resonance mass [6, 7].

9 Summary

A search for the single production of a vector-like quark T with charge $2e/3$ decaying to a top quark and a neutral scalar boson, which can be a standard model Higgs boson (H) or a new scalar boson (ϕ), has been presented. In the first case, a branching fraction of 25% is assumed for the decay $\mathrm{T} \to \mathrm{tH}$, while in the second case the T quark is assumed to decay exclusively to $\mathrm{t}\phi$. Final states where the top quark decays in the lepton+jets channel and the neutral scalar boson decays into a bottom quark-antiquark pair are considered. The analysis is based on LHC proton-proton collision data, corresponding to an integrated luminosity of $138\,\mathrm{fb}^{-1}$. No significant deviation is observed between the data and the expected background. Upper limits at 95% confidence level (CL) are set on the product of the production cross section and $\mathrm{T} \to \mathrm{t}\phi \to \mathrm{b}\ell\nu\mathrm{b}\overline{\mathrm{b}}$ branching fraction as functions of the masses of T quark (m_{T}) and of ϕ boson (m_{ϕ}), and assuming a T quark in a narrow-width approximation produced in association with a bottom quark. For an m_{ϕ} of 25 (250) GeV, values greater than 2.3 to 0.1 (14.7 to 0.3) fb are excluded at 95% CL for m_{T} between 1.0 and 3.0 (1.3 and 3.0) TeV.

These are the first exclusion limits set on the production of a single T quark decaying into a top quark and a new neutral scalar boson. The case of a vector-like quark T decaying to a top quark and a standard model Higgs boson has been studied as well, and upper limits at 95% CL are set on the product of the production cross section and $\mathrm{T} \to \mathrm{tH}$ branching fraction: values greater than 100 to 1.0 fb are excluded at 95% CL for m_{T} between 1.0 and 3.0 TeV. These results provide the best exclusion limits to date for $m_{\mathrm{T}} > 2\,\mathrm{TeV}$.

Acknowledgments

We congratulate our colleagues in the CERN accelerator departments for the excellent performance of the LHC and thank the technical and administrative staffs at CERN and at other CMS institutes for their contributions to the success of the CMS effort. In addition, we gratefully acknowledge the computing centers and personnel of the Worldwide LHC Computing Grid and other centers for delivering so effectively the computing infrastructure essential to our analyses. Finally, we acknowledge the enduring support for the construction and operation of the LHC, the CMS detector, and the supporting computing infrastructure provided by the following funding agencies: SC (Armenia), BMBWF and FWF (Austria); FNRS and FWO (Belgium); CNPq, CAPES, FAPERJ, FAPERGS, and FAPESP (Brazil); MES and BNSF (Bulgaria); CERN; CAS, MoST, and NSFC (China); MINCIENCIAS (Colombia); MSES and CSF (Croatia); RIF (Cyprus); SENESCYT (Ecuador); ERC PRG, TARISTU24-TK10 and MoER TK202 (Estonia); Academy of Finland, MEC, and HIP (Finland); CEA and CNRS/IN2P3 (France); SRNSF (Georgia); BMFTR, DFG, and HGF (Germany); GSRI (Greece); NKFIH (Hungary); DAE and DST (India); IPM (Iran); SFI (Ireland); INFN (Italy); MSIT and NRF (Republic of Korea); MES (Latvia); LMTLT (Lithuania); MOE and UM (Malaysia); BUAP, CINVESTAV, CONACYT, LNS, SEP, and UASLP-FAI (Mexico); MOS (Montenegro); MBIE (New Zealand); PAEC (Pakistan); MES, NSC, and NAWA (Poland); FCT (Portugal);MESTD (Serbia); MICIU/AEI and PCTI (Spain); MOSTR (Sri Lanka); Swiss Funding Agencies (Switzerland); MST (Taipei); MHESI (Thailand); TUBITAK and TENMAK (Türkiye); NASU (Ukraine); STFC (United Kingdom); DOE and NSF (U.S.A.).

JHEP07(2026)041

Individuals have received support from the Marie-Curie program and the European Research Council and Horizon 2020 Grant, contract Nos. 675440, 724704, 752730, 758316, 765710, 824093, 101115353, 101002207, 101001205, and COST Action CA16108 (European Union); the Leventis Foundation; the Alfred P. Sloan Foundation; the Alexander von Humboldt Foundation; the Science Committee, project no. 22rl-037 (Armenia); the Fonds pour la Formation à la Recherche dans l'Industrie et dans l'Agriculture (FRIA) and Fonds voor Wetenschappelijk Onderzoek contract No. 1228724N (Belgium); the Beijing Municipal Science & Technology Commission, No. Z191100007219010, the Fundamental Research Funds for the Central Universities, the Ministry of Science and Technology of China under Grant No. 2023YFA1605804, the Natural Science Foundation of China under Grant No. 12061141002, 12535004, and USTC Research Funds of the Double First-Class Initiative No. YD2030002017 (China); the Ministry of Education, Youth and Sports (MEYS) of the Czech Republic; the Shota Rustaveli National Science Foundation, grant FR-22-985 (Georgia); the Deutsche Forschungsgemeinschaft (DFG), among others, under Germany's Excellence Strategy – EXC 2121 "Quantum Universe" – 390833306, and under project number 400140256 – GRK2497; the Hellenic Foundation for Research and Innovation (HFRI), Project Number 2288 (Greece); the Hungarian Academy of Sciences, the New National Excellence Program – ÚNKP, the NKFIH research grants K 131991, K 133046, K 138136, K 143460, K 143477, K 146913, K 146914, K 147048, 2020-2.2.1-ED-2021-00181, TKP2021-NKTA-64, and 2021-4.1.2-NEMZ_KI-2024-00036 (Hungary); the Council of Science and Industrial Research, India; ICSC – National Research Center for High Performance Computing, Big Data and Quantum Computing, FAIR – Future Artificial Intelligence Research, and CUP I53D23001070006 (Mission 4 Component 1), funded by the NextGenerationEU program (Italy); the Latvian Council of Science; the Ministry of Education and Science, project no. 2022/WK/14, and the National Science Center, contracts Opus 2021/41/B/ST2/01369, 2021/43/B/ST2/01552, 2023/49/B/ST2/03273, and the NAWA contract BPN/PPO/2021/1/00011 (Poland); the Fundação para a Ciência e a Tecnologia, grant CEECIND/01334/2018 (Portugal); the National Priorities Research Program by Qatar National Research Fund; MICIU/AEI/10.13039/501100011033, ERDF/EU, "European Union NextGenerationEU/PRTR", and Programa Severo Ochoa del Principado de Asturias (Spain); the Chulalongkorn Academic into Its 2nd Century Project Advancement Project, the National Science, Research and Innovation Fund program IND_FF_68_369_2300_097, and the Program Management Unit for Human Resources & Institutional Development, Research and Innovation, grant B39G680009 (Thailand); the Kavli Foundation; the Nvidia Corporation; the SuperMicro Corporation; the Welch Foundation, contract C-1845; and the Weston Havens Foundation (U.S.A.).

Data Availability Statement. Release and preservation of data used by the CMS Collaboration as the basis for publications is guided by the CMS data preservation, re-use and open access policy.

Code Availability Statement. The CMS core software is publicly available on GitHub.

JHEP07(2026)041

References

[1] J.A. Aguilar-Saavedra, R. Benbrik, S. Heinemeyer and M. Pérez-Victoria, *Handbook of vectorlike quarks: Mixing and single production*, *Phys. Rev. D* **88** (2013) 094010 [arXiv:1306.0572] [INSPIRE].

[2] Y. Okada and L. Panizzi, *LHC signatures of vector-like quarks*, *Adv. High Energy Phys.* **2013** (2013) 364936 [arXiv:1207.5607] [INSPIRE].

[3] J.A. Aguilar-Saavedra, *Identifying top partners at LHC*, *JHEP* **11** (2009) 030 [arXiv:0907.3155] [INSPIRE].

[4] A. De Simone, O. Matsedonskyi, R. Rattazzi and A. Wulzer, *A First Top Partner Hunter's Guide*, *JHEP* **04** (2013) 004 [arXiv:1211.5663] [INSPIRE].

[5] O. Matsedonskyi, G. Panico and A. Wulzer, *On the Interpretation of Top Partners Searches*, *JHEP* **12** (2014) 097 [arXiv:1409.0100] [INSPIRE].

[6] M. Buchkremer, G. Cacciapaglia, A. Deandrea and L. Panizzi, *Model Independent Framework for Searches of Top Partners*, *Nucl. Phys. B* **876** (2013) 376 [arXiv:1305.4172] [INSPIRE].

[7] A. Carvalho et al., *Single production of vectorlike quarks with large width at the Large Hadron Collider*, *Phys. Rev. D* **98** (2018) 015029 [arXiv:1805.06402] [INSPIRE].

[8] O. Eberhardt et al., *Joint analysis of Higgs decays and electroweak precision observables in the Standard Model with a sequential fourth generation*, *Phys. Rev. D* **86** (2012) 013011 [arXiv:1204.3872] [INSPIRE].

[9] CMS collaboration, *Review of searches for vector-like quarks, vector-like leptons, and heavy neutral leptons in proton–proton collisions at $\sqrt{s} = 13$ TeV at the CMS experiment*, *Phys. Rept.* **1115** (2025) 570 [arXiv:2405.17605] [INSPIRE].

[10] J.A. Aguilar-Saavedra, J. Alonso-González, L. Merlo and J.M. No, *Exotic vectorlike quark phenomenology in the minimal linear σ model*, *Phys. Rev. D* **101** (2020) 035015 [arXiv:1911.10202] [INSPIRE].

[11] R. Benbrik et al., *Signatures of vector-like top partners decaying into new neutral scalar or pseudoscalar bosons*, *JHEP* **05** (2020) 028 [arXiv:1907.05929] [INSPIRE].

[12] G. Cacciapaglia, T. Flacke, M. Park and M. Zhang, *Exotic decays of top partners: mind the search gap*, *Phys. Lett. B* **798** (2019) 135015 [arXiv:1908.07524] [INSPIRE].

[13] ATLAS collaboration, *Exploration at the high-energy frontier: ATLAS Run 2 searches investigating the exotic jungle beyond the Standard Model*, *Phys. Rept.* **1116** (2025) 301 [arXiv:2403.09292] [INSPIRE].

[14] ATLAS collaboration, *Search for pair production of vector-like top quarks in events with one lepton, jets, and missing transverse momentum in $\sqrt{s} = 13$ TeV pp collisions with the ATLAS detector*, *JHEP* **08** (2017) 052 [arXiv:1705.10751] [INSPIRE].

[15] ATLAS collaboration, *Search for pair production of heavy vector-like quarks decaying to high-p_T W bosons and b quarks in the lepton-plus-jets final state in pp collisions at $\sqrt{s} = 13$ TeV with the ATLAS detector*, *JHEP* **10** (2017) 141 [arXiv:1707.03347] [INSPIRE].

[16] ATLAS collaboration, *Search for pair- and single-production of vector-like quarks in final states with at least one Z boson decaying into a pair of electrons or muons in pp collision data collected with the ATLAS detector at $\sqrt{s} = 13$ TeV*, Phys. Rev. D **98** (2018) 112010 [arXiv:1806.10555] [INSPIRE].

[17] ATLAS collaboration, *Search for pair production of heavy vector-like quarks decaying into hadronic final states in pp collisions at $\sqrt{s} = 13$ TeV with the ATLAS detector*, Phys. Rev. D **98** (2018) 092005 [arXiv:1808.01771] [INSPIRE].

[18] ATLAS collaboration, *Search for pair production of up-type vector-like quarks and for four-top-quark events in final states with multiple b-jets with the ATLAS detector*, JHEP **07** (2018) 089 [arXiv:1803.09678] [INSPIRE].

[19] ATLAS collaboration, *Combination of the searches for pair-produced vector-like partners of the third-generation quarks at $\sqrt{s} = 13$ TeV with the ATLAS detector*, Phys. Rev. Lett. **121** (2018) 211801 [arXiv:1808.02343] [INSPIRE].

[20] ATLAS collaboration, *Search for pair-produced vector-like top and bottom partners in events with large missing transverse momentum in pp collisions with the ATLAS detector*, Eur. Phys. J. C **83** (2023) 719 [arXiv:2212.05263] [INSPIRE].

[21] ATLAS collaboration, *Search for pair-production of vector-like quarks in pp collision events at $\sqrt{s} = 13$ TeV with at least one leptonically decaying Z boson and a third-generation quark with the ATLAS detector*, Phys. Lett. B **843** (2023) 138019 [arXiv:2210.15413] [INSPIRE].

[22] ATLAS collaboration, *Search for pair-production of vector-like quarks in lepton+jets final states containing at least one b-tagged jet using the Run 2 data from the ATLAS experiment*, Phys. Lett. B **854** (2024) 138743 [arXiv:2401.17165] [INSPIRE].

[23] ATLAS collaboration, *Search for pair-produced vectorlike quarks coupling to light quarks in the lepton plus jets final state using 13 TeV pp collisions with the ATLAS detector*, Phys. Rev. D **110** (2024) 052009 [arXiv:2405.19862] [INSPIRE].

[24] CMS collaboration, *Search for pair production of vector-like T and B quarks in single-lepton final states using boosted jet substructure in proton-proton collisions at $\sqrt{s} = 13$ TeV*, JHEP **11** (2017) 085 [arXiv:1706.03408] [INSPIRE].

[25] CMS collaboration, *Search for pair production of vector-like quarks in the $bW\bar{b}W$ channel from proton-proton collisions at $\sqrt{s} = 13$ TeV*, Phys. Lett. B **779** (2018) 82 [arXiv:1710.01539] [INSPIRE].

[26] CMS collaboration, *Search for vector-like T and B quark pairs in final states with leptons at $\sqrt{s} = 13$ TeV*, JHEP **08** (2018) 177 [arXiv:1805.04758] [INSPIRE].

[27] CMS collaboration, *Search for vector-like quarks in events with two oppositely charged leptons and jets in proton-proton collisions at $\sqrt{s} = 13$ TeV*, Eur. Phys. J. C **79** (2019) 364 [arXiv:1812.09768] [INSPIRE].

[28] CMS collaboration, *Search for pair production of vector-like quarks in the fully hadronic final state*, Phys. Rev. D **100** (2019) 072001 [arXiv:1906.11903] [INSPIRE].

[29] CMS collaboration, *Search for pair production of vector-like quarks in leptonic final states in proton-proton collisions at $\sqrt{s} = 13$ TeV*, JHEP **07** (2023) 020 [arXiv:2209.07327] [INSPIRE].

[30] ATLAS collaboration, *Search for single production of a vectorlike T quark decaying into a Higgs boson and top quark with fully hadronic final states using the ATLAS detector*, Phys. Rev. D **105** (2022) 092012 [arXiv:2201.07045] [INSPIRE].

JHEP07(2026)041

[31] CMS collaboration, *Search for electroweak production of a vector-like T quark using fully hadronic final states*, JHEP **01** (2020) 036 [arXiv:1909.04721] [INSPIRE].

[32] CMS collaboration, *Search for production of a single vectorlike quark decaying to tH or tZ in the all-hadronic final state in pp collisions at $\sqrt{s} = 13$ TeV*, Phys. Rev. D **110** (2024) 072012 [arXiv:2405.05071] [INSPIRE].

[33] ATLAS collaboration, *Search for single production of vector-like T quarks decaying into Ht or Zt in pp collisions at $\sqrt{s} = 13$ TeV with the ATLAS detector*, JHEP **08** (2023) 153 [arXiv:2305.03401] [INSPIRE].

[34] CMS collaboration, *Search for a vector-like quark $T' \to tH$ via the diphoton decay mode of the Higgs boson in proton-proton collisions at $\sqrt{s} = 13$ TeV*, JHEP **09** (2023) 057 [arXiv:2302.12802] [INSPIRE].

[35] ATLAS collaboration, *Search for large missing transverse momentum in association with one top-quark in proton-proton collisions at $\sqrt{s} = 13$ TeV with the ATLAS detector*, JHEP **05** (2019) 041 [arXiv:1812.09743] [INSPIRE].

[36] ATLAS collaboration, *Search for single production of vector-like quarks decaying into Wb in pp collisions at $\sqrt{s} = 13$ TeV with the ATLAS detector*, JHEP **05** (2019) 164 [arXiv:1812.07343] [INSPIRE].

[37] ATLAS collaboration, *Search for singly produced vectorlike top partners in multilepton final states with 139 fb^{-1} of pp collision data at $\sqrt{s} = 13$ TeV with the ATLAS detector*, Phys. Rev. D **109** (2024) 112012 [arXiv:2307.07584] [INSPIRE].

[38] ATLAS collaboration, *Search for new particles in final states with a boosted top quark and missing transverse momentum in proton-proton collisions at $\sqrt{s} = 13$ TeV with the ATLAS detector*, JHEP **05** (2024) 263 [arXiv:2402.16561] [INSPIRE].

[39] ATLAS collaboration, *Search for single-production of vector-like quarks decaying into Wb in the fully hadronic final state in pp collisions at $\sqrt{s} = 13$ TeV with the ATLAS detector*, JHEP **02** (2025) 075 [arXiv:2409.20273] [INSPIRE].

[40] CMS collaboration, *Search for single production of a vector-like T quark decaying to a Z boson and a top quark in proton-proton collisions at $\sqrt{s} = 13$ TeV*, Phys. Lett. B **781** (2018) 574 [arXiv:1708.01062] [INSPIRE].

[41] CMS collaboration, *Search for single production of a vector-like T quark decaying to a top quark and a Z boson in the final state with jets and missing transverse momentum at $\sqrt{s} = 13$ TeV*, JHEP **05** (2022) 093 [arXiv:2201.02227] [INSPIRE].

[42] CMS collaboration, *Search for single production of vector-like quarks decaying into a b quark and a W boson in proton-proton collisions at $\sqrt{s} = 13$ TeV*, Phys. Lett. B **772** (2017) 634 [arXiv:1701.08328] [INSPIRE].

[43] HEPData record for this analysis, (2025) DOI:10.17182/hepdata.158362.

[44] CMS collaboration, *The CMS Experiment at the CERN LHC*, 2008 JINST **3** S08004 [INSPIRE].

[45] CMS collaboration, *Development of the CMS detector for the CERN LHC Run 3*, 2024 JINST **19** P05064 [arXiv:2309.05466] [INSPIRE].

[46] CMS collaboration, *Performance of the CMS Level-1 trigger in proton-proton collisions at $\sqrt{s} = 13$ TeV*, 2020 JINST **15** P10017 [arXiv:2006.10165] [INSPIRE].

[47] CMS collaboration, *The CMS trigger system*, 2017 JINST **12** P01020 [arXiv:1609.02366] [INSPIRE].

JHEP07(2026)041

[48] CMS collaboration, *Performance of the CMS high-level trigger during LHC Run 2*, 2024 *JINST* **19** P11021 [arXiv:2410.17038] [INSPIRE].

[49] J. Alwall et al., *The automated computation of tree-level and next-to-leading order differential cross sections, and their matching to parton shower simulations*, *JHEP* **07** (2014) 079 [arXiv:1405.0301] [INSPIRE].

[50] P. Nason, *A new method for combining NLO QCD with shower Monte Carlo algorithms*, *JHEP* **11** (2004) 040 [hep-ph/0409146] [INSPIRE].

[51] S. Frixione, P. Nason and C. Oleari, *Matching NLO QCD computations with Parton Shower simulations: the POWHEG method*, *JHEP* **11** (2007) 070 [arXiv:0709.2092] [INSPIRE].

[52] S. Alioli, P. Nason, C. Oleari and E. Re, *A general framework for implementing NLO calculations in shower Monte Carlo programs: the POWHEG BOX*, *JHEP* **06** (2010) 043 [arXiv:1002.2581] [INSPIRE].

[53] S. Frixione, P. Nason and G. Ridolfi, *A Positive-weight next-to-leading-order Monte Carlo for heavy flavour hadroproduction*, *JHEP* **09** (2007) 126 [arXiv:0707.3088] [INSPIRE].

[54] H.B. Hartanto, B. Jager, L. Reina and D. Wackeroth, *Higgs boson production in association with top quarks in the POWHEG BOX*, *Phys. Rev. D* **91** (2015) 094003 [arXiv:1501.04498] [INSPIRE].

[55] R. Frederix, E. Re and P. Torrielli, *Single-top t-channel hadroproduction in the four-flavour scheme with POWHEG and aMC@NLO*, *JHEP* **09** (2012) 130 [arXiv:1207.5391] [INSPIRE].

[56] E. Re, *Single-top Wt-channel production matched with parton showers using the POWHEG method*, *Eur. Phys. J. C* **71** (2011) 1547 [arXiv:1009.2450] [INSPIRE].

[57] T. Sjöstrand et al., *An introduction to PYTHIA 8.2*, *Comput. Phys. Commun.* **191** (2015) 159 [arXiv:1410.3012] [INSPIRE].

[58] CMS collaboration, *Extraction and validation of a new set of CMS PYTHIA8 tunes from underlying-event measurements*, *Eur. Phys. J. C* **80** (2020) 4 [arXiv:1903.12179] [INSPIRE].

[59] M. Czakon and A. Mitov, *Top++: A Program for the Calculation of the Top-Pair Cross-Section at Hadron Colliders*, *Comput. Phys. Commun.* **185** (2014) 2930 [arXiv:1112.5675] [INSPIRE].

[60] M. Aliev et al., *HATHOR: HAdronic Top and Heavy quarks crOss section calculatoR*, *Comput. Phys. Commun.* **182** (2011) 1034 [arXiv:1007.1327] [INSPIRE].

[61] J.M. Lindert et al., *Precise predictions for v+jets dark matter backgrounds*, *Eur. Phys. J. C* **77** (2017) 829 [arXiv:1705.04664] [INSPIRE].

[62] G. Cacciapaglia et al., *Heavy Vector-like Top Partners at the LHC and flavour constraints*, *JHEP* **03** (2012) 070 [arXiv:1108.6329] [INSPIRE].

[63] NNPDF collaboration, *Parton distributions for the LHC Run II*, *JHEP* **04** (2015) 040 [arXiv:1410.8849] [INSPIRE].

[64] GEANT4 collaboration, *GEANT4 — A Simulation Toolkit*, *Nucl. Instrum. Meth. A* **506** (2003) 250 [INSPIRE].

[65] J. Allison et al., *Geant4 developments and applications*, *IEEE Trans. Nucl. Sci.* **53** (2006) 270 [INSPIRE].

[66] D. Contardo et al., *Technical Proposal for the Phase-II Upgrade of the CMS Detector*, CERN-LHCC-2015-010 [DOI:10.17181/CERN.VU8I.D59J] [INSPIRE].

[67] CMS collaboration, *Particle-flow reconstruction and global event description with the CMS detector*, 2017 *JINST* **12** P10003 [arXiv:1706.04965] [INSPIRE].

[68] M. Cacciari, G.P. Salam and G. Soyez, *The anti-k_t jet clustering algorithm*, *JHEP* **04** (2008) 063 [arXiv:0802.1189] [INSPIRE].

[69] M. Cacciari, G.P. Salam and G. Soyez, *FastJet User Manual*, *Eur. Phys. J. C* **72** (2012) 1896 [arXiv:1111.6097] [INSPIRE].

[70] CMS collaboration, *Pileup mitigation at CMS in 13 TeV data*, 2020 *JINST* **15** P09018 [arXiv:2003.00503] [INSPIRE].

[71] D. Bertolini, P. Harris, M. Low and N. Tran, *Pileup Per Particle Identification*, *JHEP* **10** (2014) 059 [arXiv:1407.6013] [INSPIRE].

[72] CMS collaboration, *Jet energy scale and resolution in the CMS experiment in pp collisions at 8 TeV*, 2017 *JINST* **12** P02014 [arXiv:1607.03663] [INSPIRE].

[73] CMS collaboration, *Electron and photon reconstruction and identification with the CMS experiment at the CERN LHC*, 2021 *JINST* **16** P05014 [arXiv:2012.06888] [INSPIRE].

[74] CMS collaboration, *Performance of the CMS muon detector and muon reconstruction with proton-proton collisions at $\sqrt{s} = 13$ TeV*, 2018 *JINST* **13** P06015 [arXiv:1804.04528] [INSPIRE].

[75] K. Rehermann and B. Tweedie, *Efficient Identification of Boosted Semileptonic Top Quarks at the LHC*, *JHEP* **03** (2011) 059 [arXiv:1007.2221] [INSPIRE].

[76] CMS collaboration, *Performance of missing transverse momentum reconstruction in proton-proton collisions at $\sqrt{s} = 13$ TeV using the CMS detector*, 2019 *JINST* **14** P07004 [arXiv:1903.06078] [INSPIRE].

[77] H. Qu and L. Gouskos, *ParticleNet: Jet Tagging via Particle Clouds*, *Phys. Rev. D* **101** (2020) 056019 [arXiv:1902.08570] [INSPIRE].

[78] CMS collaboration, *Measurement of the single top quark and antiquark production cross sections in the t channel and their ratio in proton-proton collisions at $\sqrt{s} = 13$ TeV*, *Phys. Lett. B* **800** (2020) 135042 [arXiv:1812.10514] [INSPIRE].

[79] Particle Data Group collaboration, *Review of particle physics*, *Phys. Rev. D* **110** (2024) 030001 [INSPIRE].

[80] CMS collaboration, *Identification of heavy-flavour jets with the CMS detector in pp collisions at 13 TeV*, 2018 *JINST* **13** P05011 [arXiv:1712.07158] [INSPIRE].

[81] E. Bols et al., *Jet Flavour Classification Using DeepJet*, 2020 *JINST* **15** P12012 [arXiv:2008.10519] [INSPIRE].

[82] CMS collaboration, *Performance of the DeepJet b tagging algorithm using 41.9 fb^{-1} of data from proton-proton collisions at 13 TeV with Phase 1 CMS detector*, CMS-DP-2018-058.

[83] T. Chen and C. Guestrin, *XGBoost: A Scalable Tree Boosting System*, arXiv:1603.02754 [DOI:10.1145/2939672.2939785] [INSPIRE].

[84] CMS collaboration, *Performance of heavy-flavour jet identification in boosted topologies in proton-proton collisions at $\sqrt{s} = 13$ TeV*, CMS-PAS-BTV-22-001.

[85] CMS collaboration, *Precision luminosity measurement in proton-proton collisions at $\sqrt{s} = 13$ TeV in 2015 and 2016 at CMS*, *Eur. Phys. J. C* **81** (2021) 800 [arXiv:2104.01927] [INSPIRE].

[86] CMS collaboration, *CMS luminosity measurement for the 2017 data-taking period at $\sqrt{s} = 13$ TeV*, CMS-PAS-LUM-17-004 [INSPIRE].

[87] CMS collaboration, *CMS luminosity measurement for the 2018 data-taking period at $\sqrt{s} = 13$ TeV*, CMS-PAS-LUM-18-002 [INSPIRE].

[88] CMS collaboration, *Measurement of the inelastic proton-proton cross section at $\sqrt{s} = 13$ TeV*, *JHEP* **07** (2018) 161 [arXiv:1802.02613] [INSPIRE].

[89] J. Butterworth et al., *PDF4LHC recommendations for LHC Run II*, *J. Phys. G* **43** (2016) 023001 [arXiv:1510.03865] [INSPIRE].

[90] CMS collaboration, *Measurement of differential cross sections for top quark pair production using the lepton+jets final state in proton-proton collisions at 13* TeV, *Phys. Rev. D* **95** (2017) 092001 [arXiv:1610.04191] [INSPIRE].

[91] R.J. Barlow and C. Beeston, *Fitting using finite Monte Carlo samples*, *Comput. Phys. Commun.* **77** (1993) 219 [INSPIRE].

[92] J.S. Conway, *Incorporating Nuisance Parameters in Likelihoods for Multisource Spectra*, in the proceedings of the *PHYSTAT 2011*, Geneva, Switzerland, January 17–20 (2011) [DOI:10.5170/CERN-2011-006.115] [arXiv:1103.0354] [INSPIRE].

[93] CMS collaboration, *The CMS Statistical Analysis and Combination Tool: Combine*, *Comput. Softw. Big Sci.* **8** (2024) 19 [arXiv:2404.06614] [INSPIRE].

[94] W. Verkerke and D.P. Kirkby, *The RooFit toolkit for data modeling*, *eConf C* **0303241** (2003) MOLT007 [physics/0306116] [INSPIRE].

[95] L. Moneta et al., *The RooStats Project*, *PoS* **ACAT2010** (2010) 057 [arXiv:1009.1003] [INSPIRE].

[96] T. Junk, *Confidence level computation for combining searches with small statistics*, *Nucl. Instrum. Meth. A* **434** (1999) 435 [hep-ex/9902006] [INSPIRE].

[97] A.L. Read, *Presentation of search results: The CL_s technique*, *J. Phys. G* **28** (2002) 2693 [INSPIRE].

[98] G. Cowan, K. Cranmer, E. Gross and O. Vitells, *Asymptotic formulae for likelihood-based tests of new physics*, *Eur. Phys. J. C* **71** (2011) 1554 [*Erratum ibid.* **73** (2013) 2501] [arXiv:1007.1727] [INSPIRE].

[99] ATLAS and CMS collaborations and LHC Higgs Combination Group, *Procedure for the LHC Higgs boson search combination in Summer 2011*, CMS-NOTE-2011-005, ATL-PHYS-PUB-2011-11 [INSPIRE].

The CMS collaboration

A. Hayrapetyan[1], V. Makarenko[1], A. Tumasyan[1,a], W. Adam[2], J.W. Andrejkovic[2], L. Benato[2], T. Bergauer[2], M. Dragicevic[2], C. Giordano[2], P.S. Hussain[2], M. Jeitler[2,b], N. Krammer[2], A. Li[2], D. Liko[2], M. Matthewman[2], I. Mikulec[2], J. Schieck[2,b], R. Schöfbeck[2,b], D. Schwarz[2], M. Shooshtari[2], M. Sonawane[2], W. Waltenberger[2], C.-E. Wulz[2,b], T. Janssen[3], H. Kwon[3], D. Ocampo Henao[3], T. Van Laer[3], P. Van Mechelen[3], J. Bierkens[4], N. Breugelmans[4], J. D'Hondt[4], S. Dansana[4], A. De Moor[4], M. Delcourt[4], F. Heyen[4], Y. Hong[4], P. Kashko[4], S. Lowette[4], I. Makarenko[4], D. Müller[4], J. Song[4], S. Tavernier[4], M. Tytgat[4,c], G.P. Van Onsem[4], S. Van Putte[4], D. Vannerom[4], B. Bilin[5], B. Clerbaux[5], A.K. Das[5], I. De Bruyn[5], G. De Lentdecker[5], H. Evard[5], L. Favart[5], P. Gianneios[5], A. Khalilzadeh[5], F.A. Khan[5], A. Malara[5], M.A. Shahzad[5], L. Thomas[5], M. Vanden Bemden[5], C. Vander Velde[5], P. Vanlaer[5], F. Zhang[5], M. De Coen[6], D. Dobur[6], G. Gokbulut[6], J. Knolle[6], D. Marckx[6], K. Skovpen[6], A.M. Tomaru[6], N. Van Den Bossche[6], J. van der Linden[6], J. Vandenbroeck[6], L. Wezenbeek[6], S. Bein[7], A. Benecke[7], A. Bethani[7], G. Bruno[7], A. Cappati[7], J. De Favereau De Jeneret[7], C. Delaere[7], A. Giammanco[7], A.O. Guzel[7], V. Lemaitre[7], J. Lidrych[7], P. Malek[7], P. Mastrapasqua[7], S. Turkcapar[7], G.A. Alves[8], M. Barroso Ferreira Filho[8], E. Coelho[8], C. Hensel[8], T. Menezes De Oliveira[8], C. Mora Herrera[8,d], P. Rebello Teles[8], M. Soeiro[8], E.J. Tonelli Manganote[8,e], A. Vilela Pereira[8,d], W.L. Aldá Júnior[9], H. Brandao Malbouisson[9], W. Carvalho[9], J. Chinellato[9,f], M. Costa Reis[9], E.M. Da Costa[9], G.G. Da Silveira[9,g], D. De Jesus Damiao[9], S. Fonseca De Souza[9], R. Gomes De Souza[9], S. S. Jesus[9], T. Laux Kuhn[9,g], M. Macedo[9], K. Mota Amarilo[9], L. Mundim[9], H. Nogima[9], J.P. Pinheiro[9], A. Santoro[9], A. Sznajder[9], M. Thiel[9], F. Torres Da Silva De Araujo[9,h], C.A. Bernardes[10,g], F. Damas[10], T.R. Fernandez Perez Tomei[10], E.M. Gregores[10], B. Lopes Da Costa[10], I. Maietto Silverio[10], P.G. Mercadante[10], S.F. Novaes[10], B. Orzari[10], Sandra S. Padula[10], V. Scheurer[10], A. Aleksandrov[11], G. Antchev[11], P. Danev[11], R. Hadjiiska[11], P. Iaydjiev[11], M. Shopova[11], G. Sultanov[11], A. Dimitrov[12], L. Litov[12], B. Pavlov[12], P. Petkov[12], A. Petrov[12], S. Keshri[13], D. Laroze[13], S. Thakur[13], W. Brooks[14], T. Cheng[15], T. Javaid[15], L. Wang[15], L. Yuan[15], Z. Hu[16], Z. Liang[16], J. Liu[16], X. Wang[16], G.M. Chen[17,i], H.S. Chen[17,i], M. Chen[17,i], Y. Chen[17], Q. Hou[17], X. Hou[17], F. Iemmi[17], C.H. Jiang[17], A. Kapoor[17,j], H. Liao[17], G. Liu[17], Z.-A. Liu[17,k], J.N. Song[17,k], S. Song[17], J. Tao[17], C. Wang[17,i], J. Wang[17], H. Zhang[17], J. Zhao[17], A. Agapitos[18], Y. Ban[18], A. Carvalho Antunes De Oliveira[18], S. Deng[18], B. Guo[18], Q. Guo[18], C. Jiang[18], A. Levin[18], C. Li[18], Q. Li[18], Y. Mao[18], S. Qian[18], S.J. Qian[18], X. Qin[18], C. Quaranta[18], X. Sun[18], D. Wang[18], J. Wang[18], H. Yang[18], M. Zhang[18], Y. Zhao[18], C. Zhou[18], S. Yang[19], Z. You[20], K. Jaffel[21], N. Lu[21], G. Bauer[22,l,m], Z. Cui[22,m], B. Li[22,n], H. Wang[22], K. Yi[22,o], J. Zhang[22], Y. Li[23], Z. Lin[24], C. Lu[24], M. Xiao[24,p], C. Avila[25], D.A. Barbosa Trujillo[25], A. Cabrera[25], C. Florez[25], J. Fraga[25], J.A. Reyes Vega[25], C. Rendón[26], M. Rodriguez[26], A.A. Ruales Barbosa[26], J.D. Ruiz Alvarez[26], N. Godinovic[27], D. Lelas[27], A. Sculac[27], M. Kovac[28], A. Petkovic[28], T. Sculac[28], P. Bargassa[29], V. Brigljevic[29], B.K. Chitroda[29], D. Ferencek[29], K. Jakovcic[29], A. Starodumov[29], T. Susa[29], A. Attikis[30], K. Christoforou[30], A. Hadjiagapiou[30],

C. Leonidou[30], C. Nicolaou[30], L. Paizanos[30], F. Ptochos[30], P.A. Razis[30], H. Rykaczewski[30], H. Saka[30], A. Stepennov[30], M. Finger[31,†], M. Finger Jr.[31], E. Ayala[32], E. Carrera Jarrin[33], S. Elgammal[34,q], A. Ellithi Kamel[34,r], M. Abdullah Al-Mashad[35], A. Hussein[35], H. Mohammed[35], K. Ehataht[36], M. Kadastik[36], T. Lange[36], C. Nielsen[36], J. Pata[36], M. Raidal[36], N. Seeba[36], L. Tani[36], A. Milieva[37], K. Osterberg[37], M. Voutilainen[37], N. Bin Norjoharuddeen[38], E. Brücken[38], F. Garcia[38], P. Inkaew[38], K.T.S. Kallonen[38], R. Kumar Verma[38], T. Lampén[38], K. Lassila-Perini[38], B. Lehtela[38], S. Lehti[38], T. Lindén[38], N.R. Mancilla Xinto[38], M. Myllymäki[38], M.m. Rantanen[38], S. Saariokari[38], N.T. Toikka[38], J. Tuominiemi[38], H. Kirschenmann[39], P. Luukka[39], H. Petrow[39], M. Besancon[40], F. Couderc[40], M. Dejardin[40], D. Denegri[40], P. Devouge[40], J.L. Faure[40], F. Ferri[40], P. Gaigne[40], S. Ganjour[40], P. Gras[40], G. Hamel de Monchenault[40], M. Kumar[40], V. Lohezic[40], J. Malcles[40], F. Orlandi[40], L. Portales[40], S. Ronchi[40], M.Ö. Sahin[40], A. Savoy-Navarro[40,s], P. Simkina[40], M. Titov[40], M. Tornago[40], R. Amella Ranz[41], F. Beaudette[41], G. Boldrini[41], P. Busson[41], C. Charlot[41], M. Chiusi[41], T.D. Cuisset[41], O. Davignon[41], A. De Wit[41], T. Debnath[41], I.T. Ehle[41], S. Ghosh[41], A. Gilbert[41], R. Granier de Cassagnac[41], L. Kalipoliti[41], M. Manoni[41], M. Nguyen[41], S. Obraztsov[41], C. Ochando[41], R. Salerno[41], J.B. Sauvan[41], Y. Sirois[41], G. Sokmen[41], L. Urda Gómez[41], A. Zabi[41], A. Zghiche[41], J.-L. Agram[42,t], J. Andrea[42], D. Bloch[42], J.-M. Brom[42], E.C. Chabert[42], C. Collard[42], G. Coulon[42], S. Falke[42], U. Goerlach[42], R. Haeberle[42], A.-C. Le Bihan[42], M. Meena[42], O. Poncet[42], G. Saha[42], P. Vaucelle[42], A. Di Florio[43], D. Amram[44], S. Beauceron[44], B. Blancon[44], G. Boudoul[44], N. Chanon[44], D. Contardo[44], P. Depasse[44], H. El Mamouni[44], J. Fay[44], S. Gascon[44], M. Gouzevitch[44], C. Greenberg[44], G. Grenier[44], B. Ille[44], E. Jourd'Huy[44], I.B. Laktineh[44], M. Lethuillier[44], B. Massoteau[44], L. Mirabito[44], A. Purohit[44], M. Vander Donckt[44], J. Xiao[44], D. Chokheli[45], I. Lomidze[45], Z. Tsamalaidze[45,u], V. Botta[46], S. Consuegra Rodríguez[46], L. Feld[46], K. Klein[46], M. Lipinski[46], D. Meuser[46], P. Nattland[46], V. Oppenländer[46], A. Pauls[46], D. Pérez Adán[46], N. Röwert[46], M. Teroerde[46], C. Daumann[47], S. Diekmann[47], A. Dodonova[47], N. Eich[47], D. Eliseev[47], F. Engelke[47], J. Erdmann[47], M. Erdmann[47], B. Fischer[47], T. Hebbeker[47], K. Hoepfner[47], F. Ivone[47], A. Jung[47], N. Kumar[47], M.y. Lee[47], F. Mausolf[47], M. Merschmeyer[47], A. Meyer[47], F. Nowotny[47], A. Pozdnyakov[47], W. Redjeb[47], H. Reithler[47], U. Sarkar[47], V. Sarkisovi[47], A. Schmidt[47], C. Seth[47], A. Sharma[47], J.L. Spah[47], V. Vaulin[47], S. Zaleski[47], M.R. Beckers[48], C. Dziwok[48], G. Flügge[48], N. Hoeflich[48], T. Kress[48], A. Nowack[48], O. Pooth[48], A. Stahl[48], A. Zotz[48], H. Aarup Petersen[49], A. Abel[49], M. Aldaya Martin[49], J. Alimena[49], S. Amoroso[49], Y. An[49], I. Andreev[49], J. Bach[49], S. Baxter[49], M. Bayatmakou[49], H. Becerril Gonzalez[49], O. Behnke[49], A. Belvedere[49], F. Blekman[49,v], K. Borras[49,w], A. Campbell[49], S. Chatterjee[49], L.X. Coll Saravia[49], G. Eckerlin[49], D. Eckstein[49], E. Gallo[49,v], A. Geiser[49], V. Guglielmi[49], M. Guthoff[49], A. Hinzmann[49], L. Jeppe[49], M. Kasemann[49], C. Kleinwort[49], R. Kogler[49], M. Komm[49], D. Krücker[49], W. Lange[49], D. Leyva Pernia[49], K.-Y. Lin[49], K. Lipka[49,x], W. Lohmann[49,y], J. Malvaso[49], R. Mankel[49], I.-A. Melzer-Pellmann[49], M. Mendizabal Morentin[49], A.B. Meyer[49], G. Milella[49], K. Moral Figueroa[49], A. Mussgiller[49], L.P. Nair[49], J. Niedziela[49], A. Nürnberg[49], J. Park[49], E. Ranken[49], A. Raspereza[49], D. Rastorguev[49], L. Rygaard[49],

M. Scham[49,z,aa], S. Schnake[49,w], P. Schütze[49], C. Schwanenberger[49,v], D. Selivanova[49], K. Sharko[49], M. Shchedrolosiev[49], D. Stafford[49], M. Torkian[49], F. Vazzoler[49], A. Ventura Barroso[49], R. Walsh[49], D. Wang[49], Q. Wang[49], K. Wichmann[49], L. Wiens[49,w], C. Wissing[49], Y. Yang[49], S. Zakharov[49], A. Zimermmane Castro Santos[49], A.R. Alves Andrade[50], M. Antonello[50], S. Bollweg[50], M. Bonanomi[50], K. El Morabit[50], Y. Fischer[50], M. Frahm[50], E. Garutti[50], A. Grohsjean[50], A.A. Guvenli[50], J. Haller[50], D. Hundhausen[50], G. Kasieczka[50], P. Keicher[50], R. Klanner[50], W. Korcari[50], T. Kramer[50], C.c. Kuo[50], F. Labe[50], J. Lange[50], A. Lobanov[50], L. Moureaux[50], A. Nigamova[50], K. Nikolopoulos[50], A. Paasch[50], K.J. Pena Rodriguez[50], N. Prouvost[50], T. Quadfasel[50], B. Raciti[50], M. Rieger[50], D. Savoiu[50], P. Schleper[50], M. Schröder[50], J. Schwandt[50], M. Sommerhalder[50], H. Stadie[50], G. Steinbrück[50], R. Ward[50], B. Wiederspan[50], M. Wolf[50], S. Brommer[51], E. Butz[51], Y.M. Chen[51], T. Chwalek[51], A. Dierlamm[51], G.G. Dincer[51], U. Elicabuk[51], N. Faltermann[51], M. Giffels[51], A. Gottmann[51], F. Hartmann[51,ab], M. Horzela[51], F. Hummer[51], U. Husemann[51], J. Kieseler[51], M. Klute[51], R. Kunnilan Muhammed Rafeek[51], O. Lavoryk[51], J.M. Lawhorn[51], A. Lintuluoto[51], S. Maier[51], M. Mormile[51], Th. Müller[51], E. Pfeffer[51], M. Presilla[51], G. Quast[51], K. Rabbertz[51], B. Regnery[51], R. Schmieder[51], N. Shadskiy[51], I. Shvetsov[51], H.J. Simonis[51], L. Sowa[51], L. Stockmeier[51], K. Tauqeer[51], M. Toms[51], B. Topko[51], N. Trevisani[51], C. Verstege[51], T. Voigtländer[51], R.F. Von Cube[51], J. Von Den Driesch[51], M. Wassmer[51], R. Wolf[51], W.D. Zeuner[51], X. Zuo[51], G. Anagnostou[52], G. Daskalakis[52], A. Kyriakis[52], G. Melachroinos[53], Z. Painesis[53], I. Paraskevas[53], N. Saoulidou[53], K. Theofilatos[53], E. Tziaferi[53], E. Tzovara[53], K. Vellidis[53], I. Zisopoulos[53], T. Chatzistavrou[54], G. Karapostoli[54], K. Kousouris[54], E. Siamarkou[54], G. Tsipolitis[54], I. Bestintzanos[55], I. Evangelou[55], C. Foudas[55], P. Katsoulis[55], P. Kokkas[55], P.G. Kosmoglou Kioseoglou[55], N. Manthos[55], I. Papadopoulos[55], J. Strologas[55], D. Druzhkin[56], C. Hajdu[56], D. Horvath[56,ac,ad], K. Márton[56], A.J. Rádl[56,ae], F. Sikler[56], V. Veszpremi[56], M. Csanád[57], K. Farkas[57], A. Fehérkuti[57,af], M.M.A. Gadallah[57,ag], Á. Kadlecsik[57], M. León Coello[57], G. Pásztor[57], G.I. Veres[57], B. Ujvari[58], G. Zilizi[58], G. Bencze[59], S. Czellar[59], J. Molnar[59], Z. Szillasi[59], T. Csorgo[60,af], F. Nemes[60,af], T. Novak[60], I. Szanyi[60,ah], S. Bansal[61], S.B. Beri[61], V. Bhatnagar[61], G. Chaudhary[61], S. Chauhan[61], N. Dhingra[61,ai], A. Kaur[61], A. Kaur[61], H. Kaur[61], M. Kaur[61], S. Kumar[61], T. Sheokand[61], J.B. Singh[61], A. Singla[61], A. Bhardwaj[62], A. Chhetri[62], B.C. Choudhary[62], A. Kumar[62], A. Kumar[62], M. Naimuddin[62], S. Phor[62], K. Ranjan[62], M.K. Saini[62], S. Acharya[63,aj], B. Gomber[63], B. Sahu[63,aj], S. Mukherjee[64], S. Baradia[65], S. Bhattacharya[65], S. Das Gupta[65], S. Dutta[65], S. Dutta[65], S. Sarkar[65], M.M. Ameen[66], P.K. Behera[66], S. Chatterjee[66], G. Dash[66], A. Dattamunsi[66], P. Jana[66], P. Kalbhor[66], S. Kamble[66], J.R. Komaragiri[66,ak], T. Mishra[66], P.R. Pujahari[66], A.K. Sikdar[66], R.K. Singh[66], P. Verma[66], S. Verma[66], A. Vijay[66], B.K. Sirasva[67], L. Bhatt[68], S. Dugad[68], G.B. Mohanty[68], M. Shelake[68], P. Suryadevara[68], A. Bala[69], S. Banerjee[69], S. Barman[69,al], R.M. Chatterjee[69], M. Guchait[69], Sh. Jain[69], A. Jaiswal[69], B.M. Joshi[69], S. Kumar[69], M. Maity[69,al], G. Majumder[69], K. Mazumdar[69], S. Parolia[69], R. Saxena[69], A. Thachayath[69], S. Bahinipati[70,am], D. Maity[70,an], P. Mal[70], K. Naskar[70,an], A. Nayak[70,an], S. Nayak[70], K. Pal[70], R. Raturi[70], P. Sadangi[70], S.K. Swain[70],

JHEP07(2026)041

S. Varghese[70,an], D. Vats[70,an], A. Alpana[71], S. Dube[71], P. Hazarika[71], B. Kansal[71], A. Laha[71], R. Sharma[71], S. Sharma[71], K.Y. Vaish[71], S. Ghosh[72], H. Bakhshiansohi[73,ao], A. Jafari[73,ap], V. Sedighzadeh Dalavi[73], M. Zeinali[73,aq], S. Bashiri[74], S. Chenarani[74,ar], S.M. Etesami[74], Y. Hosseini[74], M. Khakzad[74], E. Khazaie[74], M. Mohammadi Najafabadi[74], S. Tizchang[74,as], M. Felcini[75], M. Grunewald[75], M. Abbrescia[76a,76b], M. Barbieri[76a,76b], M. Buonsante[76a,76b], A. Colaleo[76a,76b], D. Creanza[76a,76c], N. De Filippis[76a,76c], M. De Palma[76a,76b], W. Elmetenawee[76a,76b,at], N. Ferrara[76a,76c], L. Fiore[76a], L. Longo[76a], M. Louka[76a,76b], G. Maggi[76a,76c], M. Maggi[76a], I. Margjeka[76a], V. Mastrapasqua[76a,76b], S. My[76a,76b], F. Nenna[76a,76b], S. Nuzzo[76a,76b], A. Pellecchia[76a,76b], A. Pompili[76a,76b], G. Pugliese[76a,76c], R. Radogna[76a,76b], D. Ramos[76a], A. Ranieri[76a], L. Silvestris[76a], F.M. Simone[76a,76c], Ü. Sözbilir[76a], A. Stamerra[76a,76b], D. Troiano[76a,76b], R. Venditti[76a,76b], P. Verwilligen[76a], A. Zaza[76a,76b], G. Abbiendi[77a], C. Battilana[77a,77b], D. Bonacorsi[77a,77b], P. Capiluppi[77a,77b], F.R. Cavallo[77a], M. Cuffiani[77a,77b], G.M. Dallavalle[77a], T. Diotalevi[77a,77b], F. Fabbri[77a], A. Fanfani[77a,77b], D. Fasanella[77a], P. Giacomelli[77a], C. Grandi[77a], L. Guiducci[77a,77b], S. Lo Meo[77a,au], M. Lorusso[77a,77b], L. Lunerti[77a], S. Marcellini[77a], G. Masetti[77a], F.L. Navarria[77a,77b], G. Paggi[77a,77b], A. Perrotta[77a], F. Primavera[77a,77b], A.M. Rossi[77a,77b], S. Rossi Tisbeni[77a,77b], G.P. Siroli[77a,77b], S. Costa[78a,78b,av], A. Di Mattia[78a], A. Lapertosa[78a], R. Potenza[78a,78b], A. Tricomi[78a,78b,av], J. Altork[79a,79b], P. Assiouras[79a], G. Barbagli[79a], G. Bardelli[79a], M. Bartolini[79a,79b], A. Calandri[79a,79b], B. Camaiani[79a,79b], A. Cassese[79a], R. Ceccarelli[79a], V. Ciulli[79a,79b], C. Civinini[79a], R. D'Alessandro[79a,79b], L. Damenti[79a,79b], E. Focardi[79a,79b], T. Kello[79a], G. Latino[79a,79b], P. Lenzi[79a,79b], M. Lizzo[79a], M. Meschini[79a], S. Paoletti[79a], A. Papanastassiou[79a,79b], G. Sguazzoni[79a], L. Viliani[79a], L. Benussi[80], S. Bianco[80], S. Meola[80,aw], D. Piccolo[80], M. Alves Gallo Pereira[81a], F. Ferro[81a], E. Robutti[81a], S. Tosi[81a,81b], A. Benaglia[82a], F. Brivio[82a], V. Camagni[82a,82b], F. Cetorelli[82a,82b], F. De Guio[82a,82b], M.E. Dinardo[82a,82b], P. Dini[82a], S. Gennai[82a], R. Gerosa[82a,82b], A. Ghezzi[82a,82b], P. Govoni[82a,82b], L. Guzzi[82a], M.R. Kim[82a], G. Lavizzari[82a,82b], M.T. Lucchini[82a,82b], M. Malberti[82a], S. Malvezzi[82a], A. Massironi[82a], D. Menasce[82a], L. Moroni[82a], M. Paganoni[82a,82b], S. Palluotto[82a,82b], D. Pedrini[82a], A. Perego[82a,82b], G. Pizzati[82a,82b], S. Ragazzi[82a,82b], T. Tabarelli de Fatis[82a,82b], S. Buontempo[83a], C. Di Fraia[83a,83b], F. Fabozzi[83a,83c], L. Favilla[83a,83d], A.O.M. Iorio[83a,83b], L. Lista[83a,83b,ax], P. Paolucci[83a,ab], B. Rossi[83a], P. Azzi[84a], N. Bacchetta[84a,ay], P. Bortignon[84a,84c], G. Bortolato[84a,84b], A.C.M. Bulla[84a,84c], R. Carlin[84a,84b], P. Checchia[84a], T. Dorigo[84a,az], F. Fanzago[84a], F. Gasparini[84a,84b], U. Gasparini[84a,84b], S. Giorgetti[84a], E. Lusiani[84a], M. Margoni[84a,84b], A.T. Meneguzzo[84a,84b], J. Pazzini[84a,84b], P. Ronchese[84a,84b], R. Rossin[84a,84b], M. Tosi[84a,84b], A. Triossi[84a,84b], S. Ventura[84a], M. Zanetti[84a,84b], P. Zotto[84a,84b], A. Zucchetta[84a,84b], G. Zumerle[84a,84b], A. Braghieri[85a], S. Calzaferri[85a], P. Montagna[85a,85b], M. Pelliccioni[85a], V. Re[85a], C. Riccardi[85a,85b], P. Salvini[85a], I. Vai[85a,85b], P. Vitulo[85a,85b], S. Ajmal[86a,86b], M.E. Ascioti[86a,86b], G.M. Bilei[86a], C. Carrivale[86a,86b], D. Ciangottini[86a,86b], L. Della Penna[86a,86b], L. Fanò[86a,86b], V. Mariani[86a,86b], M. Menichelli[86a], F. Moscatelli[86a,ba], A. Rossi[86a,86b], A. Santocchia[86a,86b], D. Spiga[86a], T. Tedeschi[86a,86b], C. Aimè[87a,87b], C.A. Alexe[87a,87c], P. Asenov[87a,87b], P. Azzurri[87a], G. Bagliesi[87a], R. Bhattacharya[87a], L. Bianchini[87a,87b],

JHEP07(2026)041

T. Boccali[87a], E. Bossini[87a], D. Bruschini[87a,87c], L. Calligaris[87a,87b], R. Castaldi[87a], F. Cattafesta[87a,87c], M.A. Ciocci[87a,87d], M. Cipriani[87a,87b], R. Dell'Orso[87a], S. Donato[87a,87b], R. Forti[87a,87b], A. Giassi[87a], F. Ligabue[87a,87c], A.C. Marini[87a,87b], D. Matos Figueiredo[87a], A. Messineo[87a,87b], S. Mishra[87a], V.K. Muraleedharan Nair Bindhu[87a,87b], S. Nandan[87a], F. Palla[87a], M. Riggirello[87a,87c], A. Rizzi[87a,87b], G. Rolandi[87a,87c], S. Roy Chowdhury[87a,bb], T. Sarkar[87a], A. Scribano[87a], P. Solanki[87a,87b], P. Spagnolo[87a], F. Tenchini[87a,87b], R. Tenchini[87a], G. Tonelli[87a,87b], N. Turini[87a,87d], F. Vaselli[87a,87c], A. Venturi[87a], P.G. Verdini[87a], P. Akrap[88a,88b], C. Basile[88a,88b], S.C. Behera[88a], F. Cavallari[88a], L. Cunqueiro Mendez[88a,88b], F. De Riggi[88a,88b], D. Del Re[88a,88b], E. Di Marco[88a], M. Diemoz[88a], F. Errico[88a], L. Frosina[88a,88b], R. Gargiulo[88a,88b], B. Harikrishnan[88a,88b], F. Lombardi[88a,88b], E. Longo[88a,88b], L. Martikainen[88a,88b], J. Mijuskovic[88a,88b], G. Organtini[88a,88b], N. Palmeri[88a,88b], R. Paramatti[88a,88b], S. Rahatlou[88a,88b], C. Rovelli[88a], F. Santanastasio[88a,88b], L. Soffi[88a], V. Vladimirov[88a,88b], N. Amapane[89a,89b], R. Arcidiacono[89a,89c], S. Argiro[89a,89b], M. Arneodo[89a,89c], N. Bartosik[89a,89c], R. Bellan[89a,89b], A. Bellora[89a,89b], C. Biino[89a], C. Borca[89a,89b], N. Cartiglia[89a], M. Costa[89a,89b], R. Covarelli[89a,89b], N. Demaria[89a], L. Finco[89a], M. Grippo[89a,89b], B. Kiani[89a,89b], L. Lanteri[89a,89b], F. Legger[89a], F. Luongo[89a,89b], C. Mariotti[89a], S. Maselli[89a], A. Mecca[89a,89b], L. Menzio[89a,89b], P. Meridiani[89a], E. Migliore[89a,89b], M. Monteno[89a], M.M. Obertino[89a,89b], G. Ortona[89a], L. Pacher[89a,89b], N. Pastrone[89a], M. Ruspa[89a,89c], F. Siviero[89a,89b], V. Sola[89a,89b], A. Solano[89a,89b], A. Staiano[89a], C. Tarricone[89a,89b], D. Trocino[89a], G. Umoret[89a,89b], E. Vlasov[89a,89b], R. White[89a,89b], J. Babbar[90a,90b], S. Belforte[90a], V. Candelise[90a,90b], M. Casarsa[90a], F. Cossutti[90a], K. De Leo[90a], G. Della Ricca[90a,90b], R. Delli Gatti[90a,90b], S. Dogra[91], J. Hong[91], J. Kim[91], T. Kim[91], D. Lee[91], H. Lee[91], J. Lee[91], S.W. Lee[91], C.S. Moon[91], Y.D. Oh[91], S. Sekmen[91], B. Tae[91], Y.C. Yang[91], M.S. Kim[92], G. Bak[93], P. Gwak[93], H. Kim[93], D.H. Moon[93], J. Seo[93], E. Asilar[94], F. Carnevali[94], J. Choi[94,bc], T.J. Kim[94], Y. Ryou[94], S. Ha[95], S. Han[95], B. Hong[95], J. Kim[95], K. Lee[95], K.S. Lee[95], S. Lee[95], J. Yoo[95], J. Goh[96], J. Shin[96], S. Yang[96], Y. Kang[97], H. S. Kim[97], Y. Kim[97], S. Lee[97], J. Almond[98], J.H. Bhyun[98], J. Choi[98], J. Choi[98], W. Jun[98], H. Kim[98], J. Kim[98], T. Kim[98], Y. Kim[98], Y.W. Kim[98], S. Ko[98], H. Lee[98], J. Lee[98], J. Lee[98], B.H. Oh[98], S.B. Oh[98], J. Shin[98], U.K. Yang[98], I. Yoon[98], W. Jang[99], D.Y. Kang[99], D. Kim[99], S. Kim[99], B. Ko[99], J.S.H. Lee[99], Y. Lee[99], I.C. Park[99], Y. Roh[99], I.J. Watson[99], G. Cho[100], K. Hwang[100], B. Kim[100], S. Kim[100], K. Lee[100], H.D. Yoo[100], M. Choi[101], Y. Lee[101], I. Yu[101], T. Beyrouthy[102], Y. Gharbia[102], F. Alazemi[103], K. Dreimanis[104], O.M. Eberlins[104], A. Gaile[104], C. Munoz Diaz[104], D. Osite[104], G. Pikurs[104], R. Plese[104], A. Potrebko[104], M. Seidel[104], D. Sidiropoulos Kontos[104], N.R. Strautnieks[105], M. Ambrozas[106], A. Juodagalvis[106], S. Nargelas[106], A. Rinkevicius[106], G. Tamulaitis[106], I. Yusuff[107,bd], Z. Zolkapli[107], J.F. Benitez[108], A. Castaneda Hernandez[108], A. Cota Rodriguez[108], L.E. Cuevas Picos[108], H.A. Encinas Acosta[108], L.G. Gallegos Maríñez[108], J.A. Murillo Quijada[108], L. Valencia Palomo[108], G. Ayala[109], H. Castilla-Valdez[109], H. Crotte Ledesma[109], R. Lopez-Fernandez[109], J. Mejia Guisao[109], R. Reyes-Almanza[109], A. Sánchez Hernández[109], C. Oropeza Barrera[110], M. Ramírez García[110], D.L. Ramirez Guadarrama[110], I. Bautista[111],

JHEP07(2026)041

F.E. Neri Huerta[111], I. Pedraza[111], H.A. Salazar Ibarguen[111], C. Uribe Estrada[111], I. Bubanja[112], N. Raicevic[112], P.H. Butler[113], A. Ahmad[114], M.I. Asghar[114], A. Awais[114], M.I.M. Awan[114], W.A. Khan[114], V. Avati[115], L. Forthomme[115], L. Grzanka[115], M. Malawski[115], K. Piotrzkowski[115], M. Bluj[116], M. Górski[116], M. Kazana[116], M. Szleper[116], P. Zalewski[116], K. Bunkowski[117], K. Doroba[117], A. Kalinowski[117], M. Konecki[117], J. Krolikowski[117], A. Muhammad[117], P. Fokow[118], K. Pozniak[118], W. Zabolotny[118], M. Araujo[119], D. Bastos[119], C. Beirão Da Cruz E Silva[119], A. Boletti[119], M. Bozzo[119], T. Camporesi[119], G. Da Molin[119], M. Gallinaro[119], J. Hollar[119], N. Leonardo[119], G.B. Marozzo[119], A. Petrilli[119], M. Pisano[119], J. Seixas[119], J. Varela[119], J.W. Wulff[119], P. Adzic[120], L. Markovic[120], P. Milenovic[120], V. Milosevic[120], D. Devetak[121], M. Dordevic[121], J. Milosevic[121], L. Nadderd[121], V. Rekovic[121], M. Stojanovic[121], M. Alcalde Martinez[122], J. Alcaraz Maestre[122], Cristina F. Bedoya[122], J.A. Brochero Cifuentes[122], Oliver M. Carretero[122], M. Cepeda[122], M. Cerrada[122], N. Colino[122], J. Cuchillo Ortega[122], B. De La Cruz[122], A. Delgado Peris[122], A. Escalante Del Valle[122], D. Fernández Del Val[122], J.P. Fernández Ramos[122], J. Flix[122], M.C. Fouz[122], M. Gonzalez Hernandez[122], O. Gonzalez Lopez[122], S. Goy Lopez[122], J.M. Hernandez[122], M.I. Josa[122], J. Llorente Merino[122], C. Martin Perez[122], E. Martin Viscasillas[122], D. Moran[122], C. M. Morcillo Perez[122], R. Paz Herrera[122], C. Perez Dengra[122], A. Pérez-Calero Yzquierdo[122], J. Puerta Pelayo[122], I. Redondo[122], J. Vazquez Escobar[122], J.F. de Trocóniz[123], B. Alvarez Gonzalez[124], J. Ayllon Torresano[124], A. Cardini[124], J. Cuevas[124], J. Del Riego Badas[124], D. Estrada Acevedo[124], J. Fernandez Menendez[124], S. Folgueras[124], I. Gonzalez Caballero[124], P. Leguina[124], M. Obeso Menendez[124], E. Palencia Cortezon[124], J. Prado Pico[124], A. Soto Rodríguez[124], C. Vico Villalba[124], P. Vischia[124], S. Blanco Fernández[125], I.J. Cabrillo[125], A. Calderon[125], J. Duarte Campderros[125], M. Fernandez[125], G. Gomez[125], C. Lasaosa García[125], R. Lopez Ruiz[125], C. Martinez Rivero[125], P. Martinez Ruiz del Arbol[125], F. Matorras[125], P. Matorras Cuevas[125], E. Navarrete Ramos[125], J. Piedra Gomez[125], C. Quintana San Emeterio[125], L. Scodellaro[125], I. Vila[125], R. Vilar Cortabitarte[125], J.M. Vizan Garcia[125], B. Kailasapathy[126,be], D.D.C. Wickramarathna[126], W.G.D. Dharmaratna[127,bf], K. Liyanage[127], N. Perera[127], D. Abbaneo[128], C. Amendola[128], R. Ardino[128], E. Auffray[128], J. Baechler[128], D. Barney[128], J. Bendavid[128], M. Bianco[128], A. Bocci[128], L. Borgonovi[128], C. Botta[128], A. Bragagnolo[128], C.E. Brown[128], C. Caillol[128], G. Cerminara[128], P. Connor[128], D. d'Enterria[128], A. Dabrowski[128], A. David[128], A. De Roeck[128], M.M. Defranchis[128], M. Deile[128], M. Dobson[128], P.J. Fernández Manteca[128], B.A. Fontana Santos Alves[128], W. Funk[128], A. Gaddi[128], S. Giani[128], D. Gigi[128], K. Gill[128], F. Glege[128], M. Glowacki[128], A. Gruber[128], J. Hegeman[128], J.K. Heikkilä[128], R. Hofsaess[128], B. Huber[128], T. James[128], P. Janot[128], O. Kaluzinska[128], O. Karacheban[128,y], G. Karathanasis[128], S. Laurila[128], P. Lecoq[128], C. Lourenço[128], A.-M. Lyon[128], M. Magherini[128], L. Malgeri[128], M. Mannelli[128], A. Mehta[128], F. Meijers[128], J.A. Merlin[128], S. Mersi[128], E. Meschi[128], M. Migliorini[128], F. Monti[128], F. Moortgat[128], M. Mulders[128], M. Musich[128], I. Neutelings[128], S. Orfanelli[128], F. Pantaleo[128], M. Pari[128], G. Petrucciani[128], A. Pfeiffer[128], M. Pierini[128], M. Pitt[128], H. Qu[128], D. Rabady[128], A. Reimers[128], B. Ribeiro Lopes[128], F. Riti[128],

P. Rosado[128], M. Rovere[128], H. Sakulin[128], R. Salvatico[128], S. Sanchez Cruz[128], S. Scarfi[128], M. Selvaggi[128], A. Sharma[128], K. Shchelina[128], P. Silva[128], P. Sphicas[128,bg], A.G. Stahl Leiton[128], A. Steen[128], S. Summers[128], D. Treille[128], P. Tropea[128], E. Vernazza[128], J. Wanczyk[128,bh], J. Wang[128], S. Wuchterl[128], M. Zarucki[128], P. Zehetner[128], P. Zejdl[128], G. Zevi Della Porta[128], T. Bevilacqua[129,bi], L. Caminada[129,bi], W. Erdmann[129], R. Horisberger[129], Q. Ingram[129], H.C. Kaestli[129], D. Kotlinski[129], C. Lange[129], U. Langenegger[129], L. Noehte[129,bi], T. Rohe[129], A. Samalan[129], T.K. Aarrestad[130], M. Backhaus[130], G. Bonomelli[130], C. Cazzaniga[130], K. Datta[130], P. De Bryas Dexmiers D'Archiacchiac[130,bh], A. De Cosa[130], G. Dissertori[130], M. Dittmar[130], M. Donegà[130], F. Eble[130], K. Gedia[130], F. Glessgen[130], C. Grab[130], N. Härringer[130], T.G. Harte[130], W. Lustermann[130], M. Malucchi[130], R.A. Manzoni[130], M. Marchegiani[130], L. Marchese[130], A. Mascellani[130,bh], F. Nessi-Tedaldi[130], F. Pauss[130], V. Perovic[130], B. Ristic[130], R. Seidita[130], J. Steggemann[130,bh], A. Tarabini[130], D. Valsecchi[130], R. Wallny[130], C. Amsler[131,bj], P. Bärtschi[131], F. Bilandzija[131], M.F. Canelli[131], G. Celotto[131], K. Cormier[131], M. Huwiler[131], W. Jin[131], A. Jofrehei[131], B. Kilminster[131], T.H. Kwok[131], S. Leontsinis[131], V. Lukashenko[131], A. Macchiolo[131], F. Meng[131], M. Missiroli[131], J. Motta[131], P. Robmann[131], M. Senger[131], E. Shokr[131], F. Stäger[131], R. Tramontano[131], P. Viscone[131], D. Bhowmik[132], C.M. Kuo[132], P.K. Rout[132], S. Taj[132], P.C. Tiwari[132,ak], L. Ceard[133], K.F. Chen[133], Z.g. Chen[133], A. De Iorio[133], W.-S. Hou[133], T.h. Hsu[133], Y.w. Kao[133], S. Karmakar[133], G. Kole[133], Y.y. Li[133], R.-S. Lu[133], E. Paganis[133], X.f. Su[133], J. Thomas-Wilsker[133], L.s. Tsai[133], D. Tsionou[133], H.y. Wu[133], E. Yazgan[133], C. Asawatangtrakuldee[134], N. Srimanobhas[134], Y. Maghrbi[135], D. Agyel[136], F. Dolek[136], I. Dumanoglu[136,bk], Y. Guler[136,bl], E. Gurpinar Guler[136,bl], C. Isik[136], O. Kara[136], A. Kayis Topaksu[136], Y. Komurcu[136], G. Onengut[136], K. Ozdemir[136,bm], B. Tali[136,bn], U.G. Tok[136], E. Uslan[136], I.S. Zorbakir[136], M. Yalvac[137,bo], B. Akgun[138], I.O. Atakisi[138,bp], E. Gülmez[138], M. Kaya[138,bq], O. Kaya[138,br], M.A. Sarkisla[138,bs], S. Tekten[138,bt], A. Cakir[139], K. Cankocak[139,bk,bu], S. Sen[139,bv], B. Hacisahinoglu[140], I. Hos[140,bw], B. Kaynak[140], S. Ozkorucuklu[140], O. Potok[140], H. Sert[140], C. Simsek[140], C. Zorbilmez[140], S. Cerci[141], C. Dozen[141,bx], B. Isildak[141,by], E. Simsek[141], D. Sunar Cerci[141], T. Yetkin[141,bx], A. Boyaryntsev[142], O. Dadazhanova[142], B. Grynyov[142], L. Levchuk[143], J.J. Brooke[144], A. Bundock[144], F. Bury[144], E. Clement[144], D. Cussans[144], D. Dharmender[144], H. Flacher[144], J. Goldstein[144], H.F. Heath[144], M.-L. Holmberg[144], L. Kreczko[144], S. Paramesvaran[144], L. Robertshaw[144], M.S. Sanjrani[144,ao], J. Segal[144], V.J. Smith[144], A.H. Ball[145], K.W. Bell[145], A. Belyaev[145,bz], C. Brew[145], R.M. Brown[145], D.J.A. Cockerill[145], A. Elliot[145], K.V. Ellis[145], J. Gajownik[145], K. Harder[145], S. Harper[145], J. Linacre[145], K. Manolopoulos[145], M. Moallemi[145], D.M. Newbold[145], E. Olaiya[145], D. Petyt[145], T. Reis[145], A.R. Sahasransu[145], G. Salvi[145], T. Schuh[145], C.H. Shepherd-Themistocleous[145], I.R. Tomalin[145], K.C. Whalen[145], T. Williams[145], I. Andreou[146], R. Bainbridge[146], P. Bloch[146], O. Buchmuller[146], C.A. Carrillo Montoya[146], D. Colling[146], J.S. Dancu[146], I. Das[146], P. Dauncey[146], G. Davies[146], M. Della Negra[146], S. Fayer[146], G. Fedi[146], G. Hall[146], H.R. Hoorani[146], A. Howard[146], G. Iles[146], C.R. Knight[146], P. Krueper[146], J. Langford[146], K.H. Law[146], J. León Holgado[146], E. Leutgeb[146], L. Lyons[146], A.-M. Magnan[146],

B. Maier[146], S. Mallios[146], A. Mastronikolis[146], M. Mieskolainen[146], J. Nash[146,ca], M. Pesaresi[146], P.B. Pradeep[146], B.C. Radburn-Smith[146], A. Richards[146], A. Rose[146], L. Russell[146], K. Savva[146], C. Seez[146], R. Shukla[146], A. Tapper[146], K. Uchida[146], G.P. Uttley[146], T. Virdee[146,ab], M. Vojinovic[146], N. Wardle[146], D. Winterbottom[146], J.E. Cole[147], A. Khan[147], P. Kyberd[147], I.D. Reid[147], S. Abdullin[148], A. Brinkerhoff[148], E. Collins[148], M.R. Darwish[148], J. Dittmann[148], K. Hatakeyama[148], V. Hegde[148], J. Hiltbrand[148], B. McMaster[148], J. Samudio[148], S. Sawant[148], C. Sutantawibul[148], J. Wilson[148], J.M. Hogan[149,cb], R. Bartek[150], A. Dominguez[150], S. Raj[150], A.E. Simsek[150], S.S. Yu[150], B. Bam[151], A. Buchot Perraguin[151], S. Campbell[151], R. Chudasama[151], S.I. Cooper[151], C. Crovella[151], G. Fidalgo[151], S.V. Gleyzer[151], A. Khukhunaishvili[151], K. Matchev[151], E. Pearson[151], C.U. Perez[151], P. Rumerio[151,cc], E. Usai[151], R. Yi[151], S. Cholak[152], G. De Castro[152], Z. Demiragli[152], C. Erice[152], C. Fangmeier[152], C. Fernandez Madrazo[152], E. Fontanesi[152], J. Fulcher[152], F. Golf[152], S. Jeon[152], J. O'Cain[152], I. Reed[152], J. Rohlf[152], K. Salyer[152], D. Sperka[152], D. Spitzbart[152], I. Suarez[152], A. Tsatsos[152], E. Wurtz[152], A.G. Zecchinelli[152], G. Barone[153], G. Benelli[153], D. Cutts[153], S. Ellis[153], L. Gouskos[153], M. Hadley[153], U. Heintz[153], K.W. Ho[153], T. Kwon[153], L. Lambrecht[153], G. Landsberg[153], K.T. Lau[153], J. Luo[153], S. Mondal[153], J. Roloff[153], T. Russell[153], S. Sagir[153,cd], X. Shen[153], M. Stamenkovic[153], N. Venkatasubramanian[153], S. Abbott[154], B. Barton[154], R. Breedon[154], H. Cai[154], M. Calderon De La Barca Sanchez[154], E. Cannaert[154], M. Chertok[154], M. Citron[154], J. Conway[154], P.T. Cox[154], R. Erbacher[154], O. Kukral[154], G. Mocellin[154], S. Ostrom[154], I. Salazar Segovia[154], J.S. Tafoya Vargas[154], W. Wei[154], S. Yoo[154], K. Adamidis[155], M. Bachtis[155], D. Campos[155], R. Cousins[155], A. Datta[155], G. Flores Avila[155], J. Hauser[155], M. Ignatenko[155], M.A. Iqbal[155], T. Lam[155], Y.f. Lo[155], E. Manca[155], A. Nunez Del Prado[155], D. Saltzberg[155], V. Valuev[155], R. Clare[156], J.W. Gary[156], G. Hanson[156], A. Aportela[157], A. Arora[157], J.G. Branson[157], S. Cittolin[157], S. Cooperstein[157], B. D'Anzi[157], D. Diaz[157], J. Duarte[157], L. Giannini[157], Y. Gu[157], J. Guiang[157], V. Krutelyov[157], R. Lee[157], J. Letts[157], H. Li[157], M. Masciovecchio[157], F. Mokhtar[157], S. Mukherjee[157], M. Pieri[157], D. Primosch[157], M. Quinnan[157], V. Sharma[157], M. Tadel[157], E. Vourliotis[157], F. Würthwein[157], A. Yagil[157], Z. Zhao[157], A. Barzdukas[158], L. Brennan[158], C. Campagnari[158], S. Carron Montero[158,ce], K. Downham[158], C. Grieco[158], M.M. Hussain[158], J. Incandela[158], M.W.K. Lai[158], A.J. Li[158], P. Masterson[158], J. Richman[158], S.N. Santpur[158], U. Sarica[158], R. Schmitz[158], F. Setti[158], J. Sheplock[158], D. Stuart[158], T.Á. Vámi[158], X. Yan[158], D. Zhang[158], A. Albert[159], S. Bhattacharya[159], A. Bornheim[159], O. Cerri[159], R. Kansal[159], J. Mao[159], H.B. Newman[159], G. Reales Gutiérrez[159], T. Sievert[159], M. Spiropulu[159], J.R. Vlimant[159], R.A. Wynne[159], S. Xie[159], J. Alison[160], S. An[160], M. Cremonesi[160], V. Dutta[160], E.Y. Ertorer[160], T. Ferguson[160], T.A. Gómez Espinosa[160], A. Harilal[160], A. Kallil Tharayil[160], M. Kanemura[160], C. Liu[160], P. Meiring[160], T. Mudholkar[160], S. Murthy[160], P. Palit[160], K. Park[160], M. Paulini[160], A. Roberts[160], A. Sanchez[160], W. Terrill[160], J.P. Cumalat[161], W.T. Ford[161], A. Hart[161], S. Kwan[161], J. Pearkes[161], C. Savard[161], N. Schonbeck[161], K. Stenson[161], K.A. Ulmer[161], S.R. Wagner[161], N. Zipper[161], D. Zuolo[161], J. Alexander[162], X. Chen[162], J. Dickinson[162], A. Duquette[162],

J. Fan[162], X. Fan[162], J. Grassi[162], S. Hogan[162], P. Kotamnives[162], J. Monroy[162], G. Niendorf[162], M. Oshiro[162], J.R. Patterson[162], A. Ryd[162], J. Thom[162], P. Wittich[162], R. Zou[162], L. Zygala[162], M. Albrow[163], M. Alyari[163], O. Amram[163], G. Apollinari[163], A. Apresyan[163], L.A.T. Bauerdick[163], D. Berry[163], J. Berryhill[163], P.C. Bhat[163], K. Burkett[163], J.N. Butler[163], A. Canepa[163], G.B. Cerati[163], H.W.K. Cheung[163], F. Chlebana[163], C. Cosby[163], G. Cummings[163], I. Dutta[163], V.D. Elvira[163], J. Freeman[163], A. Gandrakota[163], Z. Gecse[163], L. Gray[163], D. Green[163], A. Grummer[163], S. Grünendahl[163], D. Guerrero[163], O. Gutsche[163], R.M. Harris[163], T.C. Herwig[163], J. Hirschauer[163], V. Innocente[163], B. Jayatilaka[163], S. Jindariani[163], M. Johnson[163], U. Joshi[163], T. Klijnsma[163], B. Klima[163], K.H.M. Kwok[163], S. Lammel[163], C. Lee[163], D. Lincoln[163], R. Lipton[163], T. Liu[163], K. Maeshima[163], D. Mason[163], P. McBride[163], P. Merkel[163], S. Mrenna[163], S. Nahn[163], J. Ngadiuba[163], D. Noonan[163], S. Norberg[163], V. Papadimitriou[163], N. Pastika[163], K. Pedro[163], C. Pena[163,cf], C.E. Perez Lara[163], F. Ravera[163], A. Reinsvold Hall[163,cg], L. Ristori[163], M. Safdari[163], E. Sexton-Kennedy[163], N. Smith[163], A. Soha[163], L. Spiegel[163], S. Stoynev[163], J. Strait[163], L. Taylor[163], S. Tkaczyk[163], N.V. Tran[163], L. Uplegger[163], E.W. Vaandering[163], C. Wang[163], I. Zoi[163], C. Aruta[164], P. Avery[164], D. Bourilkov[164], P. Chang[164], V. Cherepanov[164], R.D. Field[164], C. Huh[164], E. Koenig[164], M. Kolosova[164], J. Konigsberg[164], A. Korytov[164], N. Menendez[164], G. Mitselmakher[164], K. Mohrman[164], A. Muthirakalayil Madhu[164], N. Rawal[164], S. Rosenzweig[164], V. Sulimov[164], Y. Takahashi[164], J. Wang[164], T. Adams[165], A. Al Kadhim[165], A. Askew[165], S. Bower[165], R. Goff[165], R. Hashmi[165], A. Hassani[165], R.S. Kim[165], T. Kolberg[165], G. Martinez[165], M. Mazza[165], H. Prosper[165], P.R. Prova[165], R. Yohay[165], B. Alsufyani[166], S. Butalla[166], S. Das[166], M. Hohlmann[166], M. Lavinsky[166], E. Yanes[166], M.R. Adams[167], N. Barnett[167], A. Baty[167], C. Bennett[167], R. Cavanaugh[167], R. Escobar Franco[167], O. Evdokimov[167], C.E. Gerber[167], H. Gupta[167], M. Hawksworth[167], A. Hingrajiya[167], D.J. Hofman[167], J.h. Lee[167], C. Mills[167], S. Nanda[167], G. Nigmatkulov[167], B. Ozek[167], T. Phan[167], D. Pilipovic[167], R. Pradhan[167], E. Prifti[167], P. Roy[167], T. Roy[167], N. Singh[167], M.B. Tonjes[167], N. Varelas[167], M.A. Wadud[167], J. Yoo[167], M. Alhusseini[168], D. Blend[168], K. Dilsiz[168,ch], O.K. Köseyan[168], A. Mestvirishvili[168,ci], O. Neogi[168], H. Ogul[168,cj], Y. Onel[168], A. Penzo[168], C. Snyder[168], E. Tiras[168,ck], B. Blumenfeld[169], J. Davis[169], A.V. Gritsan[169], L. Kang[169], S. Kyriacou[169], P. Maksimovic[169], M. Roguljic[169], S. Sekhar[169], M.V. Srivastav[169], M. Swartz[169], A. Abreu[170], L.F. Alcerro Alcerro[170], J. Anguiano[170], S. Arteaga Escatel[170], P. Baringer[170], A. Bean[170], Z. Flowers[170], D. Grove[170], J. King[170], G. Krintiras[170], M. Lazarovits[170], C. Le Mahieu[170], J. Marquez[170], M. Murray[170], M. Nickel[170], S. Popescu[170,cl], C. Rogan[170], C. Royon[170], S. Rudrabhatla[170], S. Sanders[170], C. Smith[170], G. Wilson[170], B. Allmond[171], N. Islam[171], A. Ivanov[171], K. Kaadze[171], Y. Maravin[171], J. Natoli[171], G.G. Reddy[171], D. Roy[171], G. Sorrentino[171], A. Baden[172], A. Belloni[172], J. Bistany-riebman[172], S.C. Eno[172], N.J. Hadley[172], S. Jabeen[172], R.G. Kellogg[172], T. Koeth[172], B. Kronheim[172], S. Lascio[172], P. Major[172], A.C. Mignerey[172], C. Palmer[172], C. Papageorgakis[172], M.M. Paranjpe[172], E. Popova[172,cm], A. Shevelev[172], L. Zhang[172], C. Baldenegro Barrera[173], H. Bossi[173], S. Bright-Thonney[173], I.A. Cali[173], Y.c. Chen[173], P.c. Chou[173], M. D'Alfonso[173], J. Eysermans[173], C. Freer[173],

G. Gomez-Ceballos[173], M. Goncharov[173], G. Grosso[173], P. Harris[173], D. Hoang[173], G.M. Innocenti[173], D. Kovalskyi[173], J. Krupa[173], L. Lavezzo[173], Y.-J. Lee[173], K. Long[173], C. Mcginn[173], A. Novak[173], M.I. Park[173], C. Paus[173], C. Reissel[173], C. Roland[173], G. Roland[173], S. Rothman[173], T.a. Sheng[173], G.S.F. Stephans[173], D. Walter[173], Z. Wang[173], B. Wyslouch[173], T. J. Yang[173], B. Crossman[174], W.J. Jackson[174], C. Kapsiak[174], M. Krohn[174], D. Mahon[174], J. Mans[174], B. Marzocchi[174], R. Rusack[174], O. Sancar[174], R. Saradhy[174], N. Strobbe[174], K. Bloom[175], D.R. Claes[175], G. Haza[175], J. Hossain[175], C. Joo[175], I. Kravchenko[175], A. Rohilla[175], J.E. Siado[175], W. Tabb[175], A. Vagnerini[175], A. Wightman[175], F. Yan[175], H. Bandyopadhyay[176], L. Hay[176], H.w. Hsia[176], I. Iashvili[176], A. Kalogeropoulos[176], A. Kharchilava[176], A. Mandal[176], M. Morris[176], D. Nguyen[176], S. Rappoccio[176], H. Rejeb Sfar[176], A. Williams[176], P. Young[176], D. Yu[176], G. Alverson[177], E. Barberis[177], J. Bonilla[177], B. Bylsma[177], M. Campana[177], J. Dervan[177], Y. Haddad[177], Y. Han[177], I. Israr[177], A. Krishna[177], M. Lu[177], N. Manganelli[177], R. Mccarthy[177], D.M. Morse[177], T. Orimoto[177], L. Skinnari[177], C.S. Thoreson[177], E. Tsai[177], D. Wood[177], S. Dittmer[178], K.A. Hahn[178], Y. Liu[178], M. Mcginnis[178], Y. Miao[178], D.G. Monk[178], M.H. Schmitt[178], A. Taliercio[178], M. Velasco[178], J. Wang[178], G. Agarwal[179], R. Band[179], R. Bucci[179], S. Castells[179], A. Das[179], A. Ehnis[179], R. Goldouzian[179], M. Hildreth[179], K. Hurtado Anampa[179], T. Ivanov[179], C. Jessop[179], A. Karneyeu[179], K. Lannon[179], J. Lawrence[179], N. Loukas[179], L. Lutton[179], J. Mariano[179], N. Marinelli[179], I. Mcalister[179], T. McCauley[179], C. Mcgrady[179], C. Moore[179], Y. Musienko[179,cn], H. Nelson[179], M. Osherson[179], A. Piccinelli[179], R. Ruchti[179], A. Townsend[179], Y. Wan[179], M. Wayne[179], H. Yockey[179], A. Basnet[180], M. Carrigan[180], R. De Los Santos[180], L.S. Durkin[180], C. Hill[180], M. Joyce[180], M. Nunez Ornelas[180], D.A. Wenzl[180], B.L. Winer[180], B. R. Yates[180], H. Bouchamaoui[181], G. Dezoort[181], P. Elmer[181], A. Frankenthal[181], M. Galli[181], B. Greenberg[181], N. Haubrich[181], K. Kennedy[181], G. Kopp[181], Y. Lai[181], D. Lange[181], A. Loeliger[181], D. Marlow[181], I. Ojalvo[181], J. Olsen[181], F. Simpson[181], D. Stickland[181], C. Tully[181], S. Malik[182], R. Sharma[182], S. Chandra[183], R. Chawla[183], A. Gu[183], L. Gutay[183], M. Jones[183], A.W. Jung[183], D. Kondratyev[183], M. Liu[183], G. Negro[183], N. Neumeister[183], G. Paspalaki[183], S. Piperov[183], N.R. Saha[183], J.F. Schulte[183], F. Wang[183], A. Wildridge[183], W. Xie[183], Y. Yao[183], Y. Zhong[183], N. Parashar[184], A. Pathak[184], E. Shumka[184], D. Acosta[185], A. Agrawal[185], C. Arbour[185], T. Carnahan[185], P. Das[185], K.M. Ecklund[185], S. Freed[185], P. Gardner[185], F.J.M. Geurts[185], T. Huang[185], I. Krommydas[185], N. Lewis[185], W. Li[185], J. Lin[185], O. Miguel Colin[185], B.P. Padley[185], R. Redjimi[185], J. Rotter[185], M. Wulansatiti[185], E. Yigitbasi[185], Y. Zhang[185], O. Bessidskaia Bylund[186], A. Bodek[186], P. de Barbaro[186,†], R. Demina[186], A. Garcia-Bellido[186], H.S. Hare[186], O. Hindrichs[186], N. Parmar[186], P. Parygin[186,cm], H. Seo[186], R. Taus[186], B. Chiarito[187], J.P. Chou[187], S.V. Clark[187], S. Donnelly[187], D. Gadkari[187], Y. Gershtein[187], E. Halkiadakis[187], C. Houghton[187], D. Jaroslawski[187], A. Kobert[187], S. Konstantinou[187], I. Laflotte[187], A. Lath[187], J. Martins[187], M. Perez Prada[187], B. Rand[187], J. Reichert[187], P. Saha[187], S. Salur[187], S. Schnetzer[187], S. Somalwar[187], R. Stone[187], S.A. Thayil[187], S. Thomas[187], J. Vora[187], D. Ally[188], A.G. Delannoy[188], S. Fiorendi[188], J. Harris[188], T. Holmes[188],

JHEP07(2026)041

A.R. Kanuganti[188], N. Karunarathna[188], J. Lawless[188], L. Lee[188], E. Nibigira[188], B. Skipworth[188], S. Spanier[188], D. Aebi[189], M. Ahmad[189], T. Akhter[189], K. Androsov[189], A. Bolshov[189], O. Bouhali[189,co], A. Cagnotta[189], V. D'Amante[189], R. Eusebi[189], P. Flanagan[189], J. Gilmore[189], Y. Guo[189], T. Kamon[189], S. Luo[189], R. Mueller[189], A. Safonov[189], N. Akchurin[190], J. Damgov[190], Y. Feng[190], N. Gogate[190], Y. Kazhykarim[190], K. Lamichhane[190], S.W. Lee[190], C. Madrid[190], A. Mankel[190], T. Peltola[190], I. Volobouev[190], E. Appelt[191], Y. Chen[191], S. Greene[191], A. Gurrola[191], W. Johns[191], R. Kunnawalkam Elayavalli[191], A. Melo[191], D. Rathjens[191], F. Romeo[191], P. Sheldon[191], S. Tuo[191], J. Velkovska[191], J. Viinikainen[191], J. Zhang[191], B. Cardwell[192], H. Chung[192], B. Cox[192], J. Hakala[192], G. Hamilton Ilha Machado[192], R. Hirosky[192], M. Jose[192], A. Ledovskoy[192], C. Mantilla[192], C. Neu[192], C. Ramón Álvarez[192], Z. Wu[192], S. Bhattacharya[193], P.E. Karchin[193], A. Aravind[194], S. Banerjee[194], K. Black[194], T. Bose[194], E. Chavez[194], S. Dasu[194], P. Everaerts[194], C. Galloni[194], H. He[194], M. Herndon[194], A. Herve[194], C.K. Koraka[194], S. Lomte[194], R. Loveless[194], A. Mallampalli[194], A. Mohammadi[194], S. Mondal[194], T. Nelson[194], G. Parida[194], L. Pétré[194], D. Pinna[194], A. Savin[194], V. Shang[194], V. Sharma[194], W.H. Smith[194], D. Teague[194], H.F. Tsoi[194], W. Vetens[194], A. Warden[194], S. Afanasiev[195], V. Alexakhin[195], Yu. Andreev[195], T. Aushev[195], D. Budkouski[195], R. Chistov[195], M. Danilov[195], T. Dimova[195], A. Ershov[195], S. Gninenko[195], I. Gorbunov[195], A. Gribushin[195], A. Kamenev[195], V. Karjavine[195], M. Kirsanov[195], V. Klyukhin[195], O. Kodolova[195,cp], V. Korenkov[195], I. Korsakov[195], A. Kozyrev[195], N. Krasnikov[195], A. Lanev[195], A. Malakhov[195], V. Matveev[195], A. Nikitenko[195,cq,cr], V. Palichik[195], V. Perelygin[195], S. Petrushanko[195], S. Polikarpov[195], O. Radchenko[195], M. Savina[195], V. Shalaev[195], S. Shmatov[195], S. Shulha[195], Y. Skovpen[195], K. Slizhevskiy[195], V. Smirnov[195], O. Teryaev[195], I. Tlisova[195], A. Toropin[195], N. Voytishin[195], A. Zarubin[195], I. Zhizhin[195], E. Boos[196], V. Bunichev[196], M. Dubinin[196,cf], L. Dudko[196], K. Ivanov[196], V. Kim[196,cn], V. Murzin[196], V. Oreshkin[196], V. Savrin[196], A. Snigirev[196], D. Sosnov[196]

[1] *Yerevan Physics Institute, Yerevan, Armenia*
[2] *Institut für Hochenergiephysik, Vienna, Austria*
[3] *Universiteit Antwerpen, Antwerpen, Belgium*
[4] *Vrije Universiteit Brussel, Brussel, Belgium*
[5] *Université Libre de Bruxelles, Bruxelles, Belgium*
[6] *Ghent University, Ghent, Belgium*
[7] *Université Catholique de Louvain, Louvain-la-Neuve, Belgium*
[8] *Centro Brasileiro de Pesquisas Fisicas, Rio de Janeiro, Brazil*
[9] *Universidade do Estado do Rio de Janeiro, Rio de Janeiro, Brazil*
[10] *Universidade Estadual Paulista, Universidade Federal do ABC, São Paulo, Brazil*
[11] *Institute for Nuclear Research and Nuclear Energy, Bulgarian Academy of Sciences, Sofia, Bulgaria*
[12] *University of Sofia, Sofia, Bulgaria*
[13] *Instituto De Alta Investigación, Universidad de Tarapacá, Casilla 7 D, Arica, Chile*
[14] *Universidad Tecnica Federico Santa Maria, Valparaiso, Chile*
[15] *Beihang University, Beijing, China*
[16] *Department of Physics, Tsinghua University, Beijing, China*
[17] *Institute of High Energy Physics, Beijing, China*
[18] *State Key Laboratory of Nuclear Physics and Technology, Peking University, Beijing, China*

JHEP07(2026)041

[19] State Key Laboratory of Nuclear Physics and Technology, Institute of Quantum Matter, South China Normal University, Guangzhou, China
[20] Sun Yat-Sen University, Guangzhou, China
[21] University of Science and Technology of China, Hefei, China
[22] Nanjing Normal University, Nanjing, China
[23] Institute of Modern Physics and Key Laboratory of Nuclear Physics and Ion-beam Application (MOE) – Fudan University, Shanghai, China
[24] Zhejiang University, Hangzhou, Zhejiang, China
[25] Universidad de Los Andes, Bogota, Colombia
[26] Universidad de Antioquia, Medellin, Colombia
[27] University of Split, Faculty of Electrical Engineering, Mechanical Engineering and Naval Architecture, Split, Croatia
[28] University of Split, Faculty of Science, Split, Croatia
[29] Institute Rudjer Boskovic, Zagreb, Croatia
[30] University of Cyprus, Nicosia, Cyprus
[31] Charles University, Prague, Czech Republic
[32] Escuela Politecnica Nacional, Quito, Ecuador
[33] Universidad San Francisco de Quito, Quito, Ecuador
[34] Academy of Scientific Research and Technology of the Arab Republic of Egypt, Egyptian Network of High Energy Physics, Cairo, Egypt
[35] Center for High Energy Physics (CHEP-FU), Fayoum University, El-Fayoum, Egypt
[36] National Institute of Chemical Physics and Biophysics, Tallinn, Estonia
[37] Department of Physics, University of Helsinki, Helsinki, Finland
[38] Helsinki Institute of Physics, Helsinki, Finland
[39] Lappeenranta-Lahti University of Technology, Lappeenranta, Finland
[40] IRFU, CEA, Université Paris-Saclay, Gif-sur-Yvette, France
[41] Laboratoire Leprince-Ringuet, CNRS/IN2P3, Ecole Polytechnique, Institut Polytechnique de Paris, Palaiseau, France
[42] Université de Strasbourg, CNRS, IPHC UMR 7178, Strasbourg, France
[43] Centre de Calcul de l'Institut National de Physique Nucleaire et de Physique des Particules, CNRS/IN2P3, Villeurbanne, France
[44] Institut de Physique des 2 Infinis de Lyon (IP2I), Villeurbanne, France
[45] Georgian Technical University, Tbilisi, Georgia
[46] RWTH Aachen University, I. Physikalisches Institut, Aachen, Germany
[47] RWTH Aachen University, III. Physikalisches Institut A, Aachen, Germany
[48] RWTH Aachen University, III. Physikalisches Institut B, Aachen, Germany
[49] Deutsches Elektronen-Synchrotron, Hamburg, Germany
[50] University of Hamburg, Hamburg, Germany
[51] Karlsruher Institut fuer Technologie, Karlsruhe, Germany
[52] Institute of Nuclear and Particle Physics (INPP), NCSR Demokritos, Aghia Paraskevi, Greece
[53] National and Kapodistrian University of Athens, Athens, Greece
[54] National Technical University of Athens, Athens, Greece
[55] University of Ioánnina, Ioánnina, Greece
[56] HUN-REN Wigner Research Centre for Physics, Budapest, Hungary
[57] MTA-ELTE Lendület CMS Particle and Nuclear Physics Group, Eötvös Loránd University, Budapest, Hungary
[58] Faculty of Informatics, University of Debrecen, Debrecen, Hungary
[59] HUN-REN ATOMKI – Institute of Nuclear Research, Debrecen, Hungary
[60] Karoly Robert Campus, MATE Institute of Technology, Gyongyos, Hungary
[61] Panjab University, Chandigarh, India
[62] University of Delhi, Delhi, India
[63] University of Hyderabad, Hyderabad, India
[64] Indian Institute of Technology Kanpur, Kanpur, India

JHEP07(2026)041

[65] Saha Institute of Nuclear Physics, HBNI, Kolkata, India
[66] Indian Institute of Technology Madras, Madras, India
[67] IISER Mohali, India, Mohali, India
[68] Tata Institute of Fundamental Research-A, Mumbai, India
[69] Tata Institute of Fundamental Research-B, Mumbai, India
[70] National Institute of Science Education and Research, An OCC of Homi Bhabha National Institute, Bhubaneswar, Odisha, India
[71] Indian Institute of Science Education and Research (IISER), Pune, India
[72] Indian Institute of Technology Hyderabad, Telangana, India
[73] Isfahan University of Technology, Isfahan, Iran
[74] Institute for Research in Fundamental Sciences (IPM), Tehran, Iran
[75] University College Dublin, Dublin, Ireland
[76a] INFN Sezione di Bari, Bari, Italy
[76b] Università di Bari, Bari, Italy
[76c] Politecnico di Bari, Bari, Italy
[77a] INFN Sezione di Bologna, Bologna, Italy
[77b] Università di Bologna, Bologna, Italy
[78a] INFN Sezione di Catania, Catania, Italy
[78b] Università di Catania, Catania, Italy
[79a] INFN Sezione di Firenze, Firenze, Italy
[79b] Università di Firenze, Firenze, Italy
[80] INFN Laboratori Nazionali di Frascati, Frascati, Italy
[81a] INFN Sezione di Genova, Genova, Italy
[81b] Università di Genova, Genova, Italy
[82a] INFN Sezione di Milano-Bicocca, Milano, Italy
[82b] Università di Milano-Bicocca, Milano, Italy
[83a] INFN Sezione di Napoli, Napoli, Italy
[83b] Università di Napoli 'Federico II', Napoli, Italy
[83c] Università della Basilicata, Potenza, Italy
[83d] Scuola Superiore Meridionale (SSM), Napoli, Italy
[84a] INFN Sezione di Padova, Padova, Italy
[84b] Università di Padova, Padova, Italy
[84c] Universita degli Studi di Cagliari, Cagliari, Italy
[85a] INFN Sezione di Pavia, Pavia, Italy
[85b] Università di Pavia, Pavia, Italy
[86a] INFN Sezione di Perugia, Perugia, Italy
[86b] Università di Perugia, Perugia, Italy
[87a] INFN Sezione di Pisa, Pisa, Italy
[87b] Università di Pisa, Pisa, Italy
[87c] Scuola Normale Superiore di Pisa, Pisa, Italy
[87d] Università di Siena, Siena, Italy
[88a] INFN Sezione di Roma, Roma, Italy
[88b] Sapienza Università di Roma, Roma, Italy
[89a] INFN Sezione di Torino, Torino, Italy
[89b] Università di Torino, Torino, Italy
[89c] Università del Piemonte Orientale, Novara, Italy
[90a] INFN Sezione di Trieste, Trieste, Italy
[90b] Università di Trieste, Trieste, Italy
[91] Kyungpook National University, Daegu, Korea
[92] Department of Mathematics and Physics – GWNU, Gangneung, Korea
[93] Chonnam National University, Institute for Universe and Elementary Particles, Kwangju, Korea
[94] Hanyang University, Seoul, Korea
[95] Korea University, Seoul, Korea

[96] *Kyung Hee University, Department of Physics, Seoul, Korea*
[97] *Sejong University, Seoul, Korea*
[98] *Seoul National University, Seoul, Korea*
[99] *University of Seoul, Seoul, Korea*
[100] *Yonsei University, Department of Physics, Seoul, Korea*
[101] *Sungkyunkwan University, Suwon, Korea*
[102] *College of Engineering and Technology, American University of the Middle East (AUM), Dasman, Kuwait*
[103] *Kuwait University – College of Science – Department of Physics, Safat, Kuwait*
[104] *Riga Technical University, Riga, Latvia*
[105] *University of Latvia (LU), Riga, Latvia*
[106] *Vilnius University, Vilnius, Lithuania*
[107] *National Centre for Particle Physics, Universiti Malaya, Kuala Lumpur, Malaysia*
[108] *Universidad de Sonora (UNISON), Hermosillo, Mexico*
[109] *Centro de Investigacion y de Estudios Avanzados del IPN, Mexico City, Mexico*
[110] *Universidad Iberoamericana, Mexico City, Mexico*
[111] *Benemerita Universidad Autonoma de Puebla, Puebla, Mexico*
[112] *University of Montenegro, Podgorica, Montenegro*
[113] *University of Canterbury, Christchurch, New Zealand*
[114] *National Centre for Physics, Quaid-I-Azam University, Islamabad, Pakistan*
[115] *AGH University of Krakow, Krakow, Poland*
[116] *National Centre for Nuclear Research, Swierk, Poland*
[117] *Institute of Experimental Physics, Faculty of Physics, University of Warsaw, Warsaw, Poland*
[118] *Warsaw University of Technology, Warsaw, Poland*
[119] *Laboratório de Instrumentação e Física Experimental de Partículas, Lisboa, Portugal*
[120] *Faculty of Physics, University of Belgrade, Belgrade, Serbia*
[121] *VINCA Institute of Nuclear Sciences, University of Belgrade, Belgrade, Serbia*
[122] *Centro de Investigaciones Energéticas Medioambientales y Tecnológicas (CIEMAT), Madrid, Spain*
[123] *Universidad Autónoma de Madrid, Madrid, Spain*
[124] *Universidad de Oviedo, Instituto Universitario de Ciencias y Tecnologías Espaciales de Asturias (ICTEA), Oviedo, Spain*
[125] *Instituto de Física de Cantabria (IFCA), CSIC-Universidad de Cantabria, Santander, Spain*
[126] *University of Colombo, Colombo, Sri Lanka*
[127] *University of Ruhuna, Department of Physics, Matara, Sri Lanka*
[128] *CERN, European Organization for Nuclear Research, Geneva, Switzerland*
[129] *PSI Center for Neutron and Muon Sciences, Villigen, Switzerland*
[130] *ETH Zurich – Institute for Particle Physics and Astrophysics (IPA), Zurich, Switzerland*
[131] *Universität Zürich, Zurich, Switzerland*
[132] *National Central University, Chung-Li, Taiwan*
[133] *National Taiwan University (NTU), Taipei, Taiwan*
[134] *High Energy Physics Research Unit, Department of Physics, Faculty of Science, Chulalongkorn University, Bangkok, Thailand*
[135] *Tunis El Manar University, Tunis, Tunisia*
[136] *Çukurova University, Physics Department, Science and Art Faculty, Adana, Turkey*
[137] *Middle East Technical University, Physics Department, Ankara, Turkey*
[138] *Bogazici University, Istanbul, Turkey*
[139] *Istanbul Technical University, Istanbul, Turkey*
[140] *Istanbul University, Istanbul, Turkey*
[141] *Yildiz Technical University, Istanbul, Turkey*
[142] *Institute for Scintillation Materials of National Academy of Science of Ukraine, Kharkiv, Ukraine*
[143] *National Science Centre, Kharkiv Institute of Physics and Technology, Kharkiv, Ukraine*
[144] *University of Bristol, Bristol, U.K.*
[145] *Rutherford Appleton Laboratory, Didcot, U.K.*
[146] *Imperial College, London, U.K.*

[147] *Brunel University, Uxbridge, U.K.*
[148] *Baylor University, Waco, Texas, U.S.A.*
[149] *Bethel University, St. Paul, Minnesota, U.S.A.*
[150] *Catholic University of America, Washington, DC, U.S.A.*
[151] *The University of Alabama, Tuscaloosa, Alabama, U.S.A.*
[152] *Boston University, Boston, Massachusetts, U.S.A.*
[153] *Brown University, Providence, Rhode Island, U.S.A.*
[154] *University of California, Davis, Davis, California, U.S.A.*
[155] *University of California, Los Angeles, California, U.S.A.*
[156] *University of California, Riverside, Riverside, California, U.S.A.*
[157] *University of California, San Diego, La Jolla, California, U.S.A.*
[158] *University of California, Santa Barbara – Department of Physics, Santa Barbara, California, U.S.A.*
[159] *California Institute of Technology, Pasadena, California, U.S.A.*
[160] *Carnegie Mellon University, Pittsburgh, Pennsylvania, U.S.A.*
[161] *University of Colorado Boulder, Boulder, Colorado, U.S.A.*
[162] *Cornell University, Ithaca, New York, U.S.A.*
[163] *Fermi National Accelerator Laboratory, Batavia, Illinois, U.S.A.*
[164] *University of Florida, Gainesville, Florida, U.S.A.*
[165] *Florida State University, Tallahassee, Florida, U.S.A.*
[166] *Florida Institute of Technology, Melbourne, Florida, U.S.A.*
[167] *University of Illinois Chicago, Chicago, Illinois, U.S.A.*
[168] *The University of Iowa, Iowa City, Iowa, U.S.A.*
[169] *Johns Hopkins University, Baltimore, Maryland, U.S.A.*
[170] *The University of Kansas, Lawrence, Kansas, U.S.A.*
[171] *Kansas State University, Manhattan, Kansas, U.S.A.*
[172] *University of Maryland, College Park, Maryland, U.S.A.*
[173] *Massachusetts Institute of Technology, Cambridge, Massachusetts, U.S.A.*
[174] *University of Minnesota, Minneapolis, Minnesota, U.S.A.*
[175] *University of Nebraska-Lincoln, Lincoln, Nebraska, U.S.A.*
[176] *State University of New York at Buffalo, Buffalo, New York, U.S.A.*
[177] *Northeastern University, Boston, Massachusetts, U.S.A.*
[178] *Northwestern University, Evanston, Illinois, U.S.A.*
[179] *University of Notre Dame, Notre Dame, Indiana, U.S.A.*
[180] *The Ohio State University, Columbus, Ohio, U.S.A.*
[181] *Princeton University, Princeton, New Jersey, U.S.A.*
[182] *University of Puerto Rico, Mayaguez, Puerto Rico, U.S.A.*
[183] *Purdue University, West Lafayette, Indiana, U.S.A.*
[184] *Purdue University Northwest, Hammond, Indiana, U.S.A.*
[185] *Rice University, Houston, Texas, U.S.A.*
[186] *University of Rochester, Rochester, New York, U.S.A.*
[187] *Rutgers, The State University of New Jersey, Piscataway, New Jersey, U.S.A.*
[188] *University of Tennessee, Knoxville, Tennessee, U.S.A.*
[189] *Texas A&M University, College Station, Texas, U.S.A.*
[190] *Texas Tech University, Lubbock, Texas, U.S.A.*
[191] *Vanderbilt University, Nashville, Tennessee, U.S.A.*
[192] *University of Virginia, Charlottesville, Virginia, U.S.A.*
[193] *Wayne State University, Detroit, Michigan, U.S.A.*
[194] *University of Wisconsin – Madison, Madison, Wisconsin, U.S.A.*
[195] *An institute or international laboratory covered by a cooperation agreement with CERN*
[196] *An institute formerly covered by a cooperation agreement with CERN*

[a] *Also at Yerevan State University, Yerevan, Armenia*
[b] *Also at TU Wien, Vienna, Austria*

JHEP07(2026)041

[c] Also at Ghent University, Ghent, Belgium
[d] Also at Universidade do Estado do Rio de Janeiro, Rio de Janeiro, Brazil
[e] Also at FACAMP – Faculdades de Campinas, Sao Paulo, Brazil
[f] Also at Universidade Estadual de Campinas, Campinas, Brazil
[g] Also at Federal University of Rio Grande do Sul, Porto Alegre, Brazil
[h] Also at The University of the State of Amazonas, Manaus, Brazil
[i] Also at University of Chinese Academy of Sciences, Beijing, China
[j] Also at China Center of Advanced Science and Technology, Beijing, China
[k] Also at University of Chinese Academy of Sciences, Beijing, China
[l] Also at School of Physics, Zhengzhou University, Zhengzhou, China
[m] Now at Henan Normal University, Xinxiang, China
[n] Also at University of Shanghai for Science and Technology, Shanghai, China
[o] Now at The University of Iowa, Iowa City, Iowa, U.S.A.
[p] Also at Center for High Energy Physics, Peking University, Beijing, China
[q] Now at British University in Egypt, Cairo, Egypt
[r] Now at Cairo University, Cairo, Egypt
[s] Also at Purdue University, West Lafayette, Indiana, U.S.A.
[t] Also at Université de Haute Alsace, Mulhouse, France
[u] Also at Another institute or international laboratory covered by a cooperation agreement with CERN
[v] Also at University of Hamburg, Hamburg, Germany
[w] Also at RWTH Aachen University, III. Physikalisches Institut A, Aachen, Germany
[x] Also at Bergische University Wuppertal (BUW), Wuppertal, Germany
[y] Also at Brandenburg University of Technology, Cottbus, Germany
[z] Also at Forschungszentrum Jülich, Juelich, Germany
[aa] Now at RWTH Aachen University, III. Physikalisches Institut A, Aachen, Germany
[ab] Also at CERN, European Organization for Nuclear Research, Geneva, Switzerland
[ac] Also at HUN-REN ATOMKI – Institute of Nuclear Research, Debrecen, Hungary
[ad] Now at Universitatea Babes-Bolyai – Facultatea de Fizica, Cluj-Napoca, Romania
[ae] Also at MTA-ELTE Lendület CMS Particle and Nuclear Physics Group, Eötvös Loránd University, Budapest, Hungary
[af] Also at HUN-REN Wigner Research Centre for Physics, Budapest, Hungary
[ag] Also at Physics Department, Faculty of Science, Assiut University, Assiut, Egypt
[ah] Also at The University of Kansas, Lawrence, Kansas, U.S.A.
[ai] Also at Punjab Agricultural University, Ludhiana, India
[aj] Also at University of Hyderabad, Hyderabad, India
[ak] Also at Indian Institute of Science (IISc), Bangalore, India
[al] Also at University of Visva-Bharati, Santiniketan, India
[am] Also at IIT Bhubaneswar, Bhubaneswar, India
[an] Also at Institute of Physics, Bhubaneswar, India
[ao] Also at Deutsches Elektronen-Synchrotron, Hamburg, Germany
[ap] Also at Isfahan University of Technology, Isfahan, Iran
[aq] Also at Sharif University of Technology, Tehran, Iran
[ar] Also at Department of Physics, University of Science and Technology of Mazandaran, Behshahr, Iran
[as] Also at Department of Physics, Faculty of Science, Arak University, ARAK, Iran
[at] Also at Helwan University, Cairo, Egypt
[au] Also at Italian National Agency for New Technologies, Energy and Sustainable Economic Development, Bologna, Italy
[av] Also at Centro Siciliano di Fisica Nucleare e di Struttura Della Materia, Catania, Italy
[aw] Also at Università degli Studi Guglielmo Marconi, Roma, Italy
[ax] Also at Scuola Superiore Meridionale, Università di Napoli 'Federico II', Napoli, Italy
[ay] Also at Fermi National Accelerator Laboratory, Batavia, Illinois, U.S.A.
[az] Also at Lulea University of Technology, Lulea, Sweden
[ba] Also at Consiglio Nazionale delle Ricerche – Istituto Officina dei Materiali, Perugia, Italy

JHEP07(2026)041

[bb] Also at UPES – University of Petroleum and Energy Studies, Dehradun, India
[bc] Also at Institut de Physique des 2 Infinis de Lyon (IP2I), Villeurbanne, France
[bd] Also at Department of Applied Physics, Faculty of Science and Technology, Universiti Kebangsaan Malaysia, Bangi, Malaysia
[be] Also at Trincomalee Campus, Eastern University, Sri Lanka, Nilaveli, Sri Lanka
[bf] Also at Saegis Campus, Nugegoda, Sri Lanka
[bg] Also at National and Kapodistrian University of Athens, Athens, Greece
[bh] Also at Ecole Polytechnique Fédérale Lausanne, Lausanne, Switzerland
[bi] Also at Universität Zürich, Zurich, Switzerland
[bj] Also at Stefan Meyer Institute for Subatomic Physics, Vienna, Austria
[bk] Also at Near East University, Research Center of Experimental Health Science, Mersin, Turkey
[bl] Also at Konya Technical University, Konya, Turkey
[bm] Also at Izmir Bakircay University, Izmir, Turkey
[bn] Also at Adiyaman University, Adiyaman, Turkey
[bo] Also at Bozok Universitetesi Rektörlügü, Yozgat, Turkey
[bp] Also at Istanbul Sabahattin Zaim University, Istanbul, Turkey
[bq] Also at Marmara University, Istanbul, Turkey
[br] Also at Milli Savunma University, Istanbul, Turkey
[bs] Also at Informatics and Information Security Research Center, Gebze/Kocaeli, Turkey
[bt] Also at Kafkas University, Kars, Turkey
[bu] Now at Istanbul Okan University, Istanbul, Turkey
[bv] Also at Hacettepe University, Ankara, Turkey
[bw] Also at Istanbul University – Cerrahpasa, Faculty of Engineering, Istanbul, Turkey
[bx] Also at Istinye University, Istanbul, Turkey
[by] Also at Yildiz Technical University, Istanbul, Turkey
[bz] Also at School of Physics and Astronomy, University of Southampton, Southampton, U.K.
[ca] Also at Monash University, Faculty of Science, Clayton, Australia
[cb] Also at Bethel University, St. Paul, Minnesota, U.S.A.
[cc] Also at Università di Torino, Torino, Italy
[cd] Also at Karamanoğlu Mehmetbey University, Karaman, Turkey
[ce] Also at California Lutheran University;, Thousand Oaks, California, U.S.A.
[cf] Also at California Institute of Technology, Pasadena, California, U.S.A.
[cg] Also at United States Naval Academy, Annapolis, Maryland, U.S.A.
[ch] Also at Bingol University, Bingol, Turkey
[ci] Also at Georgian Technical University, Tbilisi, Georgia
[cj] Also at Sinop University, Sinop, Turkey
[ck] Also at Erciyes University, Kayseri, Turkey
[cl] Also at Horia Hulubei National Institute of Physics and Nuclear Engineering (IFIN-HH), Bucharest, Romania
[cm] Now at Another institute formerly covered by a cooperation agreement with CERN
[cn] Also at Another institute formerly covered by a cooperation agreement with CERN
[co] Also at Hamad Bin Khalifa University (HBKU), Doha, Qatar
[cp] Also at Yerevan Physics Institute, Yerevan, Armenia
[cq] Also at Imperial College, London, U.K.
[cr] Now at Yerevan Physics Institute, Yerevan, Armenia
[†] Deceased

JHEP07(2026)041